Four Individually Identified Paired Dopamine Neurons Signal Taste Punishment in Larval *Drosophila*

Denise Weber[1], Katrin Vogt[2,3,4], Anton Miroschnikow[5], Michael Pankratz[5] and Andreas S. Thum[1,6*]

[1]Department of Genetics, Leipzig University, 04103 Leipzig, Germany
[2]Department of Biology, University of Konstanz, 78464 Konstanz, Germany
[3]Centre for the Advanced Study of Collective Behaviour, University of Konstanz, 78464 Konstanz, Germany
[4]Center for Brain Science, Harvard University, Cambridge, MA 02138, USA
[5]Department of Molecular Brain Physiology and Behavior, LIMES Institute, University of Bonn, Bonn, Germany
[6]German Centre for Integrative Biodiversity Research (iDiv) Halle-Jena-Leipzig, Leipzig, Germany

***Correspondence**: Andreas S. Thum, Faculty of Life Sciences, Institute of Biology, Department of Genetics, University of Leipzig, Talstraße 33, 04103 Leipzig, Germany

E-mail: andreas.thum@uni-leipzig.de

Running head: Aversive odor-taste learning in *Drosophila* larvae

Number of figures: 8 figures, one table and 7 supplemental figures

Number of pages: 67

Total word count: 16158

Keywords: *Drosophila* larvae, dopamine, olfactory, punishment, classical conditioning

Abstract

Dopaminergic neurons (DANs) carry out multiple tasks in the brain, including the transmission of information related to rewards and punishments across various animal species. They are responsible for evaluating sensory input, storing resultant associations as memory, and continuously updating them based on their relevance and reliability. Accurate comprehension of the dopaminergic system's operation necessitates an understanding of the specific functions mediated by individual DANs. To this end, our research employs *Drosophila* larvae, which possess approximately 12,000 neurons in their brains, of which only around 1% (approximately 120) are DANs.

The presynaptic projections to the mushroom body (MB) - a brain region pivotal for associative olfactory learning in insects - are limited to only eight larval dopaminergic neurons. These DANs are further subdivided into two clusters: the primary protocerebral anterior medial cluster (pPAM) comprises four cells, and the dorsolateral 1 cluster (DL1) comprises the remaining four cells. Our findings confirm previous research that demonstrates that the pPAM DANs innervating the MB's medial lobe encode for a gustatory sugar reward signal. Furthermore, we have identified four DANs in the DL1 cluster - DAN-c1, DAN-d1, DAN-f1, and DAN-g1 - each of which innervates distinct compartments of the MB peduncle, lateral appendix, and vertical lobe. Optogenetic activation of DAN-f1 and DAN-g1 alone suffices to substitute for salt punishment. Furthermore, optogenetic inhibition, calcium imaging results and electron microscopy-based reconstruction of all sensory input circuits to the four DL1 DANs demonstrate that each DAN encodes a different aspect of salt punishment, with DAN-g1 being of central importance.

To summarize, our investigation has revealed the existence of a cellular division of labor among larval DANs concerning the transmission of dopaminergic reward (pPAM cluster) and punishment signals (DL1 cluster). Individual DANs in each cluster encode for distinct but partially overlapping aspects of the teaching signal. The striking resemblance in the organizing

principle of larval DANs with that of its adult counterpart and the mammalian basal ganglion suggests that there may be a limited number of efficient neural circuit solutions available to address more complex cognitive challenges in nature.

Introduction

To cope with a constantly changing environment, animals derive benefit from learning behavioral rules that need constant adaptation and updating. To test this ability, researchers often use Pavlovian or classical conditioning experiments (Pavlov 1927), which examine an organism's capacity to form associations between sensory cues, called conditioned stimuli (CS), and rewards or punishments, referred to as aversive and appetitive unconditioned stimuli (US) or teaching signals (Gerber et al 2009, Glanzman 1995, Heisenberg 2003, Menzel 2022, Waddell 2013, Weber et al 2023b, Widmann et al 2018). Dopaminergic neurons (DANs) and other modulatory neurons mediate teaching signals that allow animals to classify a given CS into positive or negative valence based on past experience (Cognigni et al 2018, Menzel 2001, Schultz 2015, Thum & Gerber 2019, Watabe-Uchida et al 2017). For example, when a CS is paired with simultaneous activation of a specific set of DANs in the PAM cluster, larval or adult *Drosophila* subsequently perceive the odor as attractive (Burke et al 2012, Eschbach et al 2020, Liu et al 2012, Rohwedder et al 2016, Schroll et al 2006) – a similar effect was seen after optogenetic activation of DANs located in the ventral tegmental area of the mouse brain to induce conditioned place preference (Tsai et al 2009). In contrast, activation of larval DL1 DANs (Eschbach et al 2020, Schroll et al 2006, Weiglein et al 2021), adult PPL1 DANs (Aso et al 2012, Aso & Rubin 2016, Aso et al 2010, Claridge-Chang et al 2009), or DANs in the posterior tail of the stratum of mice were shown to reinforce avoidance learning (Menegas et al 2018). These examples illustrate that the dopaminergic system provides a highly conserved and fundamental neural principle of the brain, which has been retained throughout the process of evolution and executes comparable functions across diverse animal species, including even humans (Frick et al 2022).

Our research focuses on the *Drosophila* larva, an organism endowed with a relatively simple central nervous system, composing approximately 12,000 neurons (Dumstrei et al 2003, Winding et al 2023). Classical conditioning in larvae can be analyzed by stable behavioral assays (Almeida-Carvalho et al 2017, Apostolopoulou et al 2013, Scherer et al 2003, Weber

et al 2023a), in conjunction with a wealth of genetic methods for targeting single molecules and neurons (Dietzl et al 2007, Li et al 2014, Perkins et al 2015, Port et al 2020). In addition, the connectome of the brain was recently reconstructed, which enables the extraction and analysis of related wiring motifs, as well as entire learning and memory circuits (Winding et al 2023). Based on these advances, it was possible to establish a more fundamental cellular and synaptic understanding of the larval memory circuit, the mushroom body (MB) network. The MB is a higher-order parallel fiber system present in numerous invertebrate brains, including hemimetabolous as well as holometabolous insects and their larval stages (Strausfeld et al 1998, Strausfeld et al 2020). Analogous to the vertebrate cerebrum, the MB in insects is responsible for forming and maintaining associations (Heisenberg 2003, Menzel 2001, Menzel 2022, Thum & Gerber 2019, Tomer et al 2010, Waddell 2013). In the first developmental stage (L1), the larval MB comprises approximately 110 intrinsic Kenyon cells (KC) per hemisphere, which sparsely encode for conditioned stimulus (CS) information, and is dominated by olfactory input (Eichler et al 2017, Masuda-Nakagawa et al 2009).

The transmission of olfactory information from the peripheral sensory organ is achieved via only 21 olfactory receptor neurons (ORNs) per body side, which in turn send signals across 35 uni- and multiglomerular projection neurons, ultimately reaching the MB KCs (Berck et al 2016, Fishilevich et al 2005, Kreher et al 2005, Masuda-Nakagawa et al 2009, Ramaekers et al 2005). KCs receive modulatory input from 17 neurons, consisting of eight dopaminergic neurons, four octopaminergic neurons, and five neurons with unknown signaling molecule identity (Eichler et al 2017, Rohwedder et al 2016, Saumweber et al 2018, Selcho et al 2009). The DANs are divided into two clusters based on the location of their soma and related neuronal lineage, namely the the primary protocerebral anterior medial cluster (pPAM) and the dorsolateral 1 cluster (DL1) clusters. Each DAN innervates a specific and non-overlapping site in the MB, which, together with one to three output neurons, defines a distinct compartment (Eichler et al 2017). The larval MB comprises a total of 11 compartments, eight of which are defined by DAN input (Eichler et al 2017, Saumweber et al 2018). The four DANs

of the pPAM cluster (DAN-h1, DAN-i1, DAN-j1, and DAN-k1) innervate the four related compartments (h, i, j, and k) of the medial lobe and provide teaching signals for sugar rewards (Eichler et al 2017, Rohwedder et al 2016, Schleyer et al 2020). The four DANs of the DL1 cluster (DAN-c1, DAN-d1, DAN-f1, and DAN-g1) innervate the lower peduncle (c), the lateral appendix (d), the intermediate (f), and the lower vertical lobe (g) (Eichler et al 2017, Saumweber et al 2018). Previous studies have shown that the DL1 cluster is capable of mediating aversive teaching signals (Eschbach et al 2020, Schroll et al 2006, Selcho et al 2009, Weiglein et al 2021). Moreover, larvae can use a variety of natural stimuli as aversive teaching signals such as heat, electric shock, vibration, bitter substances (like quinine or caffeine), and high salt concentrations (low salt concentrations, however, are rewarding) (Aceves-Pina & Quinn 1979, Apostolopoulou et al 2016, Apostolopoulou et al 2014, Eschbach et al 2011, Gerber & Hendel 2006, Khurana et al 2009, Khurana et al 2012, Niewalda et al 2008, Pauls et al 2010, von Essen et al 2011). However, it is currently unknown if and how these natural stimuli are represented by the DL1 cluster and to what extent individual DL1 DANs are involved.

We only know that optogenetic stimulation of nociceptive sensory neurons and their downstream basin neurons has been observed to activate three out of the four DL1 DANs, namely DAN-d1, DAN-f1, and DAN-g1 (Eschbach et al 2020). Furthermore, the simultaneous presentation of odor with optogenetic activation of these three DANs has been found to elicit aversion in larvae (Eschbach et al 2020, Weiglein et al 2021). These findings suggest that the activation of DL1 DANs may induce a punishing effect during training, based on somatosensory perception. But can these four individual DANs also process other sensory modalities? Utilizing electron microscopy-based reconstruction, all first and second order input neurons of the MB, consisting of a complete set of 102 neuron pairs, were examined (Eschbach et al 2020, Winding et al 2023). The analysis identified numerous afferent sensory inputs via 20 pairs of feedforward neurons (FFNs), which can now be integrated with the published wiring diagram of all chemosensory input neurons (Miroschnikow et al 2018). This

enables a more comprehensive understanding of the distinct modes of action of the four DL1 DANs in relation to the processing of different sensory modalities.

Results

The larval dopaminergic system is functionally bipartite to convey positive and negative teaching signals

There are eight DANs in the larval brain that innervate the mushroom body that can be anatomically subdivided in four pPAM cluster and four DL1 cluster neurons (Figure 1A, supplemental Figure 1A). Three of the four pPAM cluster DANs can be labeled with the driver line R58E02-Gal4 (supplemental Figure 1A-D) (Rohwedder et al 2016). Pairing an odor presentation with simultaneous optogenetic blue light activation of R58E02 positive DANs using a mutant microbial-type rhodopsin ChR2^{XXL}, which depolarizes neurons artificially (Dawydow et al 2014), establishes an appetitive olfactory memory (supplemental Figure 1E and F) (Rohwedder et al 2016). In line with this finding, it was shown that ablation or inhibition of R58E02 positive DANs strongly reduces appetitive olfactory memory (Rohwedder et al 2016) but has no functional significance for aversive olfactory memory (supplemental Figure 1G and H) (Rohwedder et al 2016). Therefore, it can be concluded that pPAM cluster DANs are not involved in the encoding of aversive teaching signals. How are aversive teaching signals encoded?

The driver line TH-Gal4 can be used to label the four DANs of the DL1 cluster (Figure 1A and B), as well as most other DANs, except for a small subset of DANs, such as pPAM DANs and neurons in the subesophageal zone (Figure 1C and D) (Selcho et al 2009). By coupling odor presentation with simultaneous optogenetic activation of TH-Gal4 positive DANs through ChR2^{XXL}, an aversive olfactory memory can be established, which was observed after both one (Figure 1E) and three (Figure 1F) odor-DAN activation pairings. Consistent with these findings, aversive associative memory formed after one or three training cycles of odor high salt pairings were significantly reduced when DANs activity was inhibited optogenetically via GtACR2 (Figure 1G and H), a light-gated channel from the algae *Guillardia theta* (Mohammad et al 2017). Please note that in these experiments salt has to be added during the test to

initiate the recall of the aversive memory (indicated as red test plates, Figure 1) (Gerber & Hendel 2006, Schleyer et al 2015). Previous studies have shown that the larva only recalls aversive odor-high salt memory when tested in the presence of the teaching signal. The prevailing explanation suggests that the larva engages in memory-based search during the test, but only if the memory content can be used in a beneficial way (Schleyer et al 2015).

From our results, we infer a division of labor at the level of DANs toward the MB. On the one hand, pPAM neurons mediate a dopaminergic appetitive teaching signal, and on the other hand, DL1 neurons convey a dopaminergic aversive teaching signal. Nevertheless, the findings related to DL1 DANs necessitate additional validation as the TH-Gal4 driver line used in the experiment labels approximately 120 cells, thus limiting the ability to draw cell-specific conclusions.

Anatomical single-cell analysis of DL1 DANs

In an earlier investigation, we conducted a screening of several thousand Gal4 lines in order to construct a high-resolution atlas of the mushroom body at the cellular level via light microscopy (Figure 2A) (Saumweber et al 2018). A subsequent reconstruction of the wiring diagram of the entire MB at the electron microscopic level encompassed not only individual neurons but all synaptic connections (Eichler et al 2017). Utilizing this anatomical work, we identified a total of 102 Gal4 lines featuring MB extrinsic neuron expression patterns. These lines were subjected to intersectional strategies in order to restrict expression patterns to single neurons (Eschbach et al 2020, Saumweber et al 2018). For the present study, we employed eight split-Gal4 lines chosen from this set, as they contained only one or two DANs of the DL1 cluster.

DAN-c1 was specifically labeled by SS02160 (Figure 2B), DAN-d1 by MB328B and MB143B (Figure 2C and supplement Figure 2A), DAN-f1 by SS02180 and MB145B (Figure 2D and

supplement Figure 2B) and DAN-g1 by SS01716 (Figure 2E). In addition, we used the split-Gal4 lines MB065B (Figure 2F), SS01702 (Figure 2G) and MB054B (Figure H-K) that specifically labeled DAN-c1/DAN-f1, DAN-c1/MBIN-e1 or DAN-f1/DAN-g1, respectively. For our evaluation we crossed each split-Gal4 line with the reporter strain UAS-mCD8::GFP;mb247-LexA,lexAop-mRFP (Burke et al 2012) that allowed us to monitor the expression pattern (green) in the background of a MB specific reference staining (magenta). Our results confirm the reported specificity even despite the use of different reporter lines and lacking antibody staining (Eschbach et al 2020), as we analyzed only endogenous GFP expression using a more cautious and faster whole mount staining protocol (see Material and Methods). Having established anatomical validity, we subsequently employed these lines to explore the physiological response of each DAN within the DL1 cluster to sugar and salt stimuli. For the purpose of analyzing DAN-d1 and DAN-f1, we limited our investigation to the split-Gal4 lines MB328B and SS02180 as these lines displayed more robust expression levels.

Physiological single-cell analysis of DL1 DANs

In order to investigate how high salt teaching signals are represented at the level of individual DL1 DANs, we conducted calcium imaging experiments using a microfluidic chip on intact and immobilized larvae, as previously described (Si et al 2019). We expressed GCaMP6m under the control of four different split-Gal4 lines specific to DL1 DANs (SS02160 (DAN-c1), MB328B (DAN-d1), SS02180 (DAN-f1), and SS01716 (DAN-g1)), as well as the pPAM specific R58E02-Gal4, and exposed the larvae to solutions containing 100 mM salt, 1 M salt, and also to 500 mM fructose. Our results showed that while none of the cells were activated by 100 mM salt, DAN-c1, DAN-d1, and DAN-g1 responded to 1 M salt (Figure 3A, B, and D). Conversely, pPAM DANs showed a reduced signal in response to 100mM and 1 M salt (Figure 3E). Both DAN-c1 and pPAM DANs showed a calcium increase in response to 500 mM fructose (Figure 3A and E). Although DAN-f1 did not respond to either salt concentration, a

reduction in the calcium signal was seen for 500 mM fructose (Figure 3C). Overall, these results provide support for the functional division of the larval dopaminergic system at the physiological level, where most DL1 neurons are activated by high salt concentrations, with one exception inhibited by fructose. In contrast, pPAM cluster neurons display the opposite response, being inhibited by high salt concentrations and strongly activated by fructose.

Behavioral single-cell analysis of DL1 DANs

We employed split-Gal4 lines SS02160 (DAN-c1), MB328B (DAN-d1), SS02180 (DAN-f1), and SS01716 (DAN-g1) to express the apoptosis proteins Hid and Reaper, resulting in the ablation of the respective individual DL1 DANs. The ablated animals were subjected to the aversive odor-high salt memory assay, using one (Figure 4A-D) and three training cycles (Figure 4E-H). We utilized two different training protocols to differentiate between the effects on short-term memory (STM) and anesthesia-resistant memory (ARM), as previous studies have demonstrated that larvae exhibit both after one training cycle, whereas only ARM is present after three training cycles (Widmann et al 2016). However, to our surprise, we found that the ablation of individual DL1 DANs had no effect on aversive olfactory memories in any of the eight experiments conducted (Figure 4A-H). For DAN-d1 and DAN-f1 we verified these results by using the additional split-Gal4 lines MB143B and MB145B (supplemental Figure 2). In addition, ablation of DAN-d1, DAN-f1 and DAN-g1 individually did not have any impact on odor-quinine and odor-fructose memories established after one cycle training (supplemental Figures 3 and 4). Moreover, MB input neurons that are not dopaminergic (OAN-a1, a2, MBIN-b1, b2, and OAN-e1) were also found to have no relevant effect (supplemental Figure 5). These results suggest that although DL1 DANs respond to high salt concentrations (Figure 3), they are not individually necessary for mediating the aversive teaching signal. It appears that the aversive teaching signal is distributed among multiple cells, indicating the presence of some redundancy. Alternatively, it is possible that there are developmental compensatory

effects for DL1 cluster DANs, allowing the remaining three neurons (or other cells) to take over the function of the ablated one.

The combination of DAN-f1 and DAN-g1 is required to establish aversive odor-high salt memories

In order to investigate a possible redundancy among DANs, we proceeded by using split-Gal4 lines MB054B (DAN-f1/DAN-g1), MB065B (DAN-c1/DAN-f1), and SS01702 (DAN-c1/MBIN-e1) to express apoptosis proteins Hid and Reaper. This approach selectively ablated either two DL1 DANs or one DL1 DAN and another MB input neuron with unknown neurotransmitter identity. It should be noted that no additional split-Gal4 lines are presently available for further DL1 DAN combinations or the complete DL1 cluster. We then subjected the larvae to the aversive odor-high salt memory assay, using one (Figure 5A-C) and three (Figure 5D-F) training cycles. Only larvae with ablated DAN-f1/DAN-g1 exhibited significantly reduced aversive olfactory memory after one cycle training (Figure 5A). No memory reduction was observed when ablating DAN-c1/DAN-f1 or DAN-c1/MBIN-e1 (Figure 5B and C). Ablation of all three sets of neurons, including MB054B, had no effect on aversive olfactory memory after three training cycles (Figure 5D-F). To ascertain the independence of the DAN-f1/DAN-g1 neuron-mediated impairment of aversive olfactory memory after one cycle training from the specific odors used, hexyl acetate and benzaldehyde were employed instead of amyl acetate and benzaldehyde. The results of these experiments confirmed the previous findings, as ablation of DAN-f1/DAN-g1 neurons significantly reduced aversive odor-high salt memory after one cycle training (Figure 5G), but not after three cycles (Figure 5J). Innate olfactory and gustatory behavior was not impaired by DAN-f1/DAN-g1 ablation (supplemental Figure 6).

Subsequently, we investigated the selectivity of DAN-f1/DAN-g1 neurons concerning the nature of the aversive teaching stimulus. To this end, we utilized quinine as an aversive teaching signal, a stimulus that has been demonstrated to be learnable by the larva, as

evidenced by previous studies (Apostolopoulou et al 2014, El-Keredy et al 2012). Removal of the DAN-f1/DAN-g1 neurons using the split-Gal4 line MB054B had no effect on aversive odor-quinine memory independent of the number of training cycles (Figure 5H and K). Furthermore, ablation of DAN-f1/DAN-g1 did not alter appetitive odor-fructose memories after one or three training cycles (Figure 5I and L). Therefore, the DL1 DAN-f1/DAN-g1 combination seems to be specifically required for aversive odor-high salt memory.

Individual DL1 DANs can instruct an aversive high salt memory

In order to determine if the activation of individual DL1 DANs signals the natural high salt punishment, we conducted a one training trial learning experiment using ChR2^{XXL} to artificially activate DAN-c1, DAN-d1, DAN-f1, DAN-g1, and the combination of DAN-f1/DAN-g1. We used split-Gal4 lines SS02160, MB328B, SS02180, SS01716, and MB054B, respectively (Figure 6). Our approach suggests that an aversive olfactory memory induced by optogenetic activation of a single DL1-DAN, when recalled on a salt plate, corresponds to a natural aversive odor-high salt memory.

Simultaneously activating DAN-f1/DAN-g1 positive DANs via ChR2^{XXL} during an odor presentation establishes an aversive olfactory memory (Figure 6E and F). These results are comparable to those observed for TH-Gal4 (as shown in Figure 1E and F). Additionally, this memory is observed after one (Figure 6E) and three training cycles (Figure 6F). Furthermore, single-cell analysis indicates that individual activation of DAN-f1 and DAN-g1, but not of DAN-d1 and DAN-c1 (please note that experimental animals are different from zero and significantly different to one control), can induce an aversive odor-high salt memory (Figure 6A-D). In summary, these results suggest that DAN-f1 and DAN-g1 encode aspects of the natural aversive high salt teaching signal under the conditions that we tested.

Individual DL1 DANs are acutely necessary to establish aversive odor-high salt memories

Next, we examined the extent to which the individual DL1 DANs are acutely required for the transmission of a functional aversive teaching signal. We have already shown that the combination of DAN-f1/DAN-g1 is required for aversive odor-high salt memory (Figure 5A and G). However, in these experiments DANs were removed during the entire development, which may have led to compensatory mechanisms or side effects.

To overcome this limitation, we left the individual DL1 DANs intact during embryonic and larval development and used GtACR2 to selectively inhibit DAN activity only during training, thus isolating the teaching signals from other DAN functions. Optogenetic inhibition of DAN-f1/DAN-g1 resulted in a reduced aversive odor-high salt memory. This was the case after one training cycle (Figure 7E) and three training cycles (Figure 7F). Thus, the learning deficit in this experiment was more pronounced than after ablation of these two DL1 DANs throughout development (Figure 5D). Optogenetic inhibition of individual DL1 DANs showed no effect on aversive odor-high salt memories (Figure 7A-C), except for DAN-g1 that led to a small but significant reduction (Figure 7D).

A synaptic reconstruction of all chemosensory inputs for each individual DL1 and pPAM DAN.

Given the apparent cellular division of labor of DANs for reward and punishment teaching signals through the pPAM and DL1 cluster (Figure 1 and supplement Figure 1) and even qualitative differences between individual DL1 DANs (Figure 3-7), since not all DANs code equally for the punishment teaching signal, the question arises as to how this may result from the respective cellular and synaptic connectivity. Therefore, we compared the input wiring diagrams of the pPAM and DL1 clusters and their individual DANs by mapping the synaptic connections from sensory neurons - to interneurons - to individual DANs, using the full larval brain EM volume (Figure 8, supplemental Figure 7) (Eschbach et al 2020, Miroschnikow et al

2018, Winding et al 2023). We found that DAN-c1, DAN-d1, DAN-f1, and DAN-g1 (black circle) get input from 1, 6, 6 or 11 sensory-to-DAN interneurons (orange circle), respectively (Figure 8A). The number of sensory neurons (numbers in colored circuits below) varies between 3, 42, 35 and 9. There is no direct input from sensory neurons onto DL1 DANs. DAN-c1 receives only very weak internal and gustatory input, while DAN-d1 and DAN-g1 have an overall stronger and additional input from somatosensory neurons. In addition, DAN-d1, as well as DAN-f1, receive information from olfactory and thermosensory neurons (Figure 8D). DAN-f1 and DAN-g1 get 17% and 11% of their entire input from these sensory-to-DAN interneurons. For DAN-d1 and DAN-c1 these number were lower (5% and 1%, respectively). In general, DL1 DANs get additional input from other upstream neurons (US) that are not directly linked to sensory neurons (grey circles; between 17% and 37%), as well as MB KCs (purple circles; between 36% and 49%) as well as a bit of MBON feedback (dark-red circle; between 1% and 2%). Please note that we restricted our analysis on direct sensory-to-DANs interneurons (single hop analysis) and did not expand the analysis onto two hop or three hop connections to keep the evaluation restricted to the shortest paths from sensory neurons to DANs. For the pPAM DANs we found the same general connectivity principles as for DL1 DANs regarding input from MBONs, KCs, and non-sensory upstream neurons. Please note that the DAN-h1 neuron is not present at the early L1 EM brain volume and thus cannot be included in this evaluation (Figure 8B). In contrast, however, it is striking that pPAM DANs seem to get input from more interneurons connected to the sensory system (up to 101 for DAN-j1) signaling additional internal somatosensory and CO_2 information. A closer inspection of the sensory-to-DAN interneurons showed that 27 of the 35 neurons are specifically innervating only DL1 or pPAM DANs (Figure 8C). Only 8 out of 35 interneurons connect to both clusters. Based on a calculated hub score sensory-to-DAN interneurons pair 1 (FB2IN-12) and pair 5 (FFN-21) were likely most significant for instructing DL1 DANs with sensory information. Whereas pairs 10 (FFN-17) and 11 (FFN-12) were – based on connectivity – most important in instructing DL1 and pPAM DANs. For the three pPAM DANs sensory-to-DAN interneuron pairs 16, 17, 18, 19 and 20 resulted in the highest hub scores (FFN-37, FFN-4, FFN-5, FFN-18 and FB-4).

The difference in cellular connectivity of DL1 and pPAM DANs is also reflected in different local input brain hubs: axo-dendritic synapses of sensory-to-DAN interneurons with DL1 DANs formed a characteristic hook-shape in the superior protocerebrum; in contrast, pPAM DANs get synaptic input from sensory-to-DAN interneurons in the anterior inferior protocerebrum (Figure 8F).

Discussion

A functional assignment for individual DANs of the DL1 cluster in their ability to encode a salt punishment teaching signal.

The discovery of DL1 neurons as aversive teaching signal mediators in larval *Drosophila* complements previous findings that demonstrate the sufficiency of four DANs from the pPAM cluster as an appetitive reinforcement signal in these animals (Rohwedder et al 2016). This dichotomy demonstrates an organizational principle shared by adult *Drosophila* and larvae (Aso et al 2012, Aso & Rubin 2016, Aso et al 2010, Burke et al 2012, Claridge-Chang et al 2009, Das et al 2014, Huetteroth et al 2015, Liu et al 2012, Schleyer et al 2020, Schroll et al 2006, Selcho et al 2009, Weiglein et al 2021, Yamagata et al 2015), despite a significant reduction in cell numbers. The principle appears to apply to mammals as well (Groessl et al 2018, Lammel et al 2012, Menegas et al 2018, Schultz 2015). But how do individual neurons contribute to the teaching signal of the complete cluster? Is the signal evenly distributed across multiple cells, supporting the mass action hypothesis, or do individual DANs specifically encode for the salt stimulus, as posited by the labeled line hypothesis? Our results show that the four DL1 DANs perform this function in a mixture of both forms. There is no unique labeled line because both ablation of each individual DAN (Figure 4) and the acute optogenetic inhibition (Figure 7) do not abolish the odor-high salt memory. The teaching signal is combinatorically encoded within the DL1 cluster, yet its distribution among the four DANs is non-uniform and relies heavily on the functionalities of DAN-g1 and DAN-f1, (Table 1, Figure 5-7). Each DAN possesses a distinct identity, which is defined by its specific, albeit partially overlapping, neuronal input circuitry and physiological response to salt (Table 1, Figure 3 and 8).

We speculate that DAN-c1 activity does not encode a taste-specific teaching signal. It rather transmits preprocessed information from the higher brain to build a more integrated aversive memory, such as a general alert memory or a state-dependent memory as this particular cell

is only weakly connected to three sensory neurons via a single sensor-to-DAN interneuron and is activated by both positive and negative tastes. DAN-d1 activity appears to have a negligible impact on the formation of odor-high salt memories in the paradigms we tested. Even though the neuron responds to high salt concentrations and receives input from 42 sensory neurons via six sensor-to-DAN interneurons, its activity did not induce an aversive memory and was not found to be essential for odor-high salt memory. Nonetheless, it is possible that DAN-d1 could instruct other salt-dependent memory types, established after non-associative training, second-order conditioning, or reversal learning (Kacsoh et al 2015, Konig et al 2019, Mancini et al 2019, Paranjpe et al 2012, Tabone & de Belle 2011, Yamada et al 2023). Indeed, other studies involving optogenetic training using CsChrimson and one-odor training suggest that DAN-d1 activation can even instruct aversive olfactory memory in larvae (Eschbach et al 2020, Weiglein et al 2021). In combination, DAN-f1 activity and DAN-g1 seem to have a crucial function in high salt punishment. DAN-f1 is inhibited by sugar and obtains input from 35 sensory neurons through six sensor-to-DAN interneurons. Despite persistent and current suppression of activity having no impact on the retention of a memory related to a high salt stimulus, DAN-f1 activity can instruct the formation of such a memory. This discovery is consistent with previous research, although their experimental designs differ from our own in the test situation (Eschbach et al 2020, Weiglein et al 2021). Consequently, it is plausible that DAN-f1 activity encodes for a teaching signal that carries additional information beyond high salt. It is evident that DAN-g1 exerts the most potent effect. Following exposure to high salt, this cell becomes active, is crucial for the formation of an odor-high salt memory and can even establish it. Additionally, it receives extensive sensory input from nine neurons through 11 distinct interneurons. Therefore, DAN-g1 is the only cell of the DL1 cluster that satisfies all prerequisites to independently encode the high salt teaching signal. In summary, the DL1 cluster appears to be arranged in a judicious functional configuration. The instructive signal is encoded by a mere four cells, with the requisite redundancy to preclude loss of function in the event of single-cell failure. Nevertheless, the cells manifest variation, thereby covering different and cumulative characteristics of stimulation.

The functioning of the DL1 cluster DANs as a multimodal node for punishment.

Larvae, of course, perceive not only high salt concentrations as punishing, but also other sensory stimuli such as bitter substances (quinines and caffeine), electric shock, temperature, mechanosensory input (vibration), and light (Aceves-Pina & Quinn 1979, Apostolopoulou et al 2016, Apostolopoulou et al 2014, Eschbach et al 2011, Gerber & Hendel 2006, Khurana et al 2012, Pauls et al 2010, von Essen et al 2011). However, the extent to which the DL1 cluster is involved in coding for most of these aversive teaching signals remains unclear. Currently, comparisons at the level of DANs can only be made for sensory inputs that are dependent on high salt or mechanosensation. Interestingly, similar to high salt concentrations, somatosensory information can also result in the establishment of aversive olfactory memory in larvae (Eschbach et al 2020). The transmission of these somatosensory teaching signals is orchestrated by mechanosensory neurons from the chordotonal organs, class IV multidendritic nociceptive neurons distributed along the body, and multisensory basin neurons (Hwang et al 2007, Jovanic et al 2016, Ohyama et al 2015, Tracey et al 2003). The connectome revealed that these mechanosensory neurons also link to the DL1 cluster through three to four interneurons and elicit the activation of DAN-d1, DAN-f1, and DAN-g1 (Eschbach et al 2020). Upon comparing the interneurons that relay high salt and mechanosensory information to the DL1 cluster, six pairs of interneurons are of critical significance, respectively. These pairs include FFN-20, FB2N-12, FB2N-19, FFN-23, FFN-29, and FB2N-15 for mechanosensory information (Eschbach et al 2020), and FB2N-12, FB2N-18, FB2IN-11, FB2IN-6, FFN-21, and FFN-24 for high salt concentrations (Figure 8; supplemental Figure 7, rightmost column). Interestingly, only one pair of interneurons - FB2N12 - is shared between the two types of information and the other five types are specific to the sensory modality. The wiring patterns of DAN input neurons exhibit a notable consistency, with a limited number of neurons dedicated to a specific sensory modality, and single neurons shared across different modalities. This results in a unique combination of cellular codes that are partly redundant and

partly specific for the four DL1 DANs. While certain DANs may hold greater significance for a particular information, such as DAN-d1 for somatosensory information, the DAN-g1 cell appears to play a general central role for encoding an aversive teaching signal. DAN-g1 responds to all aversive stimuli tested thus far and its activity has proven informative for all aversive memories analyzed to date. In order to gain a deeper comprehension of the processing of diverse sensory modalities in the larval brain, it is crucial to broaden the analytical framework presented in our work to encompass visual stimuli, various bitter substances, and temperature stimuli.

However, the overall depiction presented above of the information flow and processing of DL1 DANs is an oversimplification. Indeed, DL1 and pPAM DANs are among the most complex and highly recurrent neurons in the brain (Winding et al 2023). This exceptional level of recurrent connectivity enables DANs to provide high-dimensional feedback, which enables them to encode a diverse range of features and engage in parallel computations. Such computations can guide a working memory, contain feedback from neurons that integrate both learned and innate values, and receive long-range feedback from descending neurons that encode motor commands; all in addition to polysynaptic feedforward inputs from the entire set of sensory modalities.

A cellular comparison of DAN function across *Drosophila* metamorphosis

A recent study conducted by Truman and colleagues explored the integration, or lack thereof, of individual input and output neurons from the larval MB into the adult network following metamorphosis (Truman et al 2023). The study demonstrated that while all four DANs of the pPAM cluster perished, three out of the four cells from the DL1 cluster persisted as part of the adult MB circuitry. Only DAN-f1 altered its innervation in the adult brain, relocating from the larval MB to the adult superior medial protocerebrum. In contrast, DAN-c1, DAN-d1, and DAN-

g1 maintained their function as MB DANs in the adult system, identified as PPL1-γ1pedc, PPL1-γ2α'1, and PPL1-γ1, respectively.

Due to the lack of appropriate genetic tools, data on the function of PPL1-γ1 is scarce (Aso et al 2014). Therefore, a functional comparison between larval and adult DANs is only possible for the DAN-c1/PPL1-γ1pedc and DAN-d1/PPL1-γ2α'1 combination. Intriguingly, the adult PPL1 cluster has a bipartite functional organization (Schnitzer et al 2023, Vrontou et al 2021). Embryonic-born DAN-c1/PPL1-γ1pedc, DAN-d1/PPL1-γ2α'1, and DAN-g1/PPL1-γ1 exhibit sustained activity and respond to various sensory stimuli, including electric shock, temperature, or bitter taste, that can instruct short lasting aversive memories (Aso et al 2012, Aso & Rubin 2016, Aso et al 2010, Claridge-Chang et al 2009, Das et al 2014, Galili et al 2014, Kirkhart & Scott 2015, Schnitzer et al 2023, Tomchik 2013, Villar et al 2022, Vrontou et al 2021). Conversely, rewarding stimuli such as sugar water inhibit the spiking of these DANs (Schnitzer et al 2023), possibly with involvement of NPF (Krashes et al 2009). The remaining three PPL1-DANs (PPL1-α′3, PPL1-α′2α2, PPL1-α3), which do not have a larval history, exhibit more sporadic firing and do not respond as strongly to environmental stimuli (Vrontou et al 2021). With repeated conditioning cycles, these slower-acting PPL1-DANs become less inhibited by feedback from the short-term learning units DAN-c1/PPL1-γ1pedc and DAN-d1/PPL1-γ2α'1, enabling them to respond more strongly to sensory input (Schnitzer et al 2023). Thus, the MB circuit in adult flies features a feedback loop involving embryonic-born DAN-c1/PPL1-γ1pedc and DAN-d1/PPL1-γ2α'1, which connect to output neurons that in turn communicate with later-born PPL1-α′3, PPL1-α′2α2, and PPL1-α3 DANs. This loop serves to facilitate short-term memory formation and regulate the induction of long-term memory traces, ensuring that only repeated and reliable associations are retained (Schnitzer et al 2023). Despite the massive reorganization of the mushroom body, the basic function of DAN-c1/PPL1-γ1pedc and DAN-d1/PPL1-γ2α'1, mediating punishment teaching signals that instruct short-term memories, remains the same. Evidence indicates that the underlying molecular signaling pathways maintain their identity and kinetics throughout development,

with larval and adult interstimulus interval curves for DAN-d1/PPL1-γ2α'1 being almost identical (Aso & Rubin 2016, Schnitzer et al 2023, Weiglein et al 2021).

During adulthood, PPL1-DANs are responsible for numerous other functions, including innate olfactory responses, suppression of appetite memory in response to nutritional status, pre-exposure learning, memory reconsolidation, and forgetting (Berry et al 2015, Berry et al 2018, Felsenberg et al 2017, Jacob et al 2021, Krashes et al 2009, McCurdy et al 2021, Placais et al 2012, Siju et al 2020, Tian et al 2016, Vrontou et al 2021). Additionally, they are involved in various behaviors like locomotion and sleep (Berry et al 2015). An open question is whether larval DL1 DANs encode these same functions to a similar extent. Our study establishes a fundamental framework that can be leveraged to investigate this issue. Considering the numerical simplicity of the larval nervous system, the available genetic tools, and the complete connectome, it may be possible to attain an understanding of the larval dopaminergic system at the level of single cells and single synapses. It is plausible that nature has a limited number of effective neural circuit solutions for complex cognitive and behavioral problems, such as the remarkable ability of brains to learn from a small number of examples. Therefore, comprehending the larval dopaminergic system may provide insight into the shared circuit motifs that exist across the animal kingdom.

Materials and Methods

Fly Strains

Flies were raised and maintained on *Drosophila* standard food at 25°C, 60-80% relative humidity and a 14/7-hour light/dark cycle. For anatomical analysis, UAS-mCD8::GFP (Bloomington stock center no. 32194) (Selcho et al 2009), UAS-mCD8::GFP;mb247-LexA,lexAop-mRFP/TM3,Sb (Burke et al 2012) and UAS-mCD8::GFP;nSyb-LexA,lexAop-mRFP/TM6B (Burke et al 2012, Riabinina et al 2015) were used to analyze the morphology of DANs. For behavioral experiments, UAS-hid,rpr (Abbott & Lengyel 1991, White et al 1996), UAS-GtACR2 (Mohammad et al 2017) (Bloomington stock center no. 92984) and UAS-ChR2^{XXL} (Dawydow et al 2014) (Bloomington stock center no. 58374) were used to ablate or optogenetically silence or activate neurons by blue light (470 nm). UAS-GCaMP6m (Chen et al 2013) (Bloomington stock center no. 42748) flies were used for Ca^{2+}-imaging experiments. The Gal4 strains TH-Gal4 (Friggi-Grelin et al 2003) and R58E02-Gal4 (Rohwedder et al 2016) (Bloomington stock center no. 41347) were used to manipulate different sets of DANs. Split-Gal4 lines MB054B, MB065B, MB328B, MB143B, MB145B, SS02160, SS02180, SS01716, SS01958, SS21716, SS24765, SS01702 (Eschbach et al 2020, Pfeiffer et al 2010, Saumweber et al 2018) were used for anatomical, physiological and behavioral experiments. *w*^{1118} flies (Bloomington stock center no. 3605) were used to obtain heterozygous driver and effector control groups. See supplementary table 1 for more information.

Anatomical Analysis

Immunostaining

To confirm expression patterns of R58E02-Gal4 and TH-Gal4, flies were crossed to UAS-mCD8::GFP and raised at 25°C for seven days before dissection. Third instar larvae (wandering stage) were put on ice and dissected in PBS (Phosphate Buffered Saline; Sigma

Aldrich, cat. no. P4417). Brains were fixed in 4% formaldehyde solution (in PBS, Thermo Scientific, cat. no. 047392.9M) for 20 minutes at room temperature. After eight rinses in PBT (PBS with 3% Triton X-100, Sigma Aldrich, cat. no. X100), brains were blocked with 5% normal goat serum (NGS, Sigma Aldrich, cat. no. G9023) in PBT for 1 hour at room temperature and incubated for 48 hours with primary antibodies at 4°C. Before application of the secondary antibodies for at least 24 hours at 4°C, brains were washed seven times with PBT. After that, larval brains were again washed eight times with PBT and mounted on poly-L-lysin-coated coverslips (Janelia FlyLight DPX mounting receipt: https://www.janelia.org/project-team/flylight/protocols), dehydrated through a series of increasing concentrations of ethanol and cleared three times for 5 minutes in xylene (Sigma Aldrich, cat. no. 247642). At the end, larval brains were mounted in DPX mounting medium (dibutyl phthalate in xylene, Sigma Aldrich, cat. no. 06522) and left to rest in the dark for at least 24 hours before imaging. Primary antibodies were: rat anti-N-Cadherin (1:50; Hybridoma, cat. no. DN-Ex #8-s), rabbit anti-GFP (1:1000; Life Technologies, cat. no. A6455) and mouse 4F3 anti-DLG (1:200; Hybridoma, cat. no. 4F3 anti-discs large). Secondary antibodies were: goat anti-rat Alexa Fluor 647 (1:500, for anti-N-Cadherin, Life Technologies, cat. no. A21247), goat anti-rabbit Alexa Fluor 488 (1:500, for anti-GFP, Life Technologies, cat. no. A11008) and goat anti-mouse Alexa Fluor 568 (1:500, for anti-DLG, Life Technologies, cat. no. A10037).

Native fluorescence

For native fluorescence, we used a previously described protocol for adult flies (Pitman et al 2011) and adapted it to larvae. All split-Gal4 lines were crossed to UAS-mCD8::GFP;mb247-LexA,lexAop-mRFP/TM3,Sb, while split-Gal4 line MB054B was additionally crossed to UAS-mCD8::GFP;nSyb-LexA,lexAop-mRFP/TM6B and raised at 25°C for seven days. Third instar larvae (wandering stage) were put on ice and dissected in PBS. Brains were fixed under vacuum in 4% formaldehyde solution (in PBS) for 25 minutes at room temperature. After five

washes in PBT (PBS with 3% Triton X-100), larval brains were rinsed twice directly and once for 10 minutes under vacuum in PBS at room temperature. Samples were mounted on poly-L-lysin-coated coverslips and embedded in Vectashield (Vector Laboratories, cat. no. H-1000-10). Slides were stored in the dark and cold for at least 24 hours before imaging.

Confocal microscopy

Confocal microscopy was conducted on a Zeiss LSM800 confocal laser scanning microscope with ZEN 2.3 software. All images were projected and adjusted with ImageJ (Fiji is just ImageJ, Version 1.53c, Java 1.8.0_172 (64-bit)). Final Figures were arranged and labeled in Affinity Publisher 2.1.1.

Functional Imaging and microfluidics

For larval imaging experiments, adult flies were transferred to larvae collection cages (Genesee Scientific) containing grape juice agar plates and 180 mg of fresh yeast paste per cage. Flies were allowed to lay eggs on the agar plate for 1–2 days before the plate was removed for collection of larvae. Calcium imaging experiments were performed in L1 larvae (2 days AEL). We used a previously described method for microfluidic delivery of chemicals in aqueous form with simultaneous imaging of calcium activity in intact larvae (Si et al 2019). All experiments used an 8-channel microfluidic chip equipped with a vacuum port to stabilize the animal's head. The same tastants were used as in the behavioral experiments (NaCl: VWR Chemicals, cat. no. 27810.364; D-Fructose: Sigma Aldrich cat. no. 47740). Stimuli consisted of 5-10 s pulses interleaved with 15 s water washout periods. An L1 larva was washed with deionized water and loaded into the microfluidic device using a 1 mL syringe filled with Triton X-100 (0.1% [v/v]) solution. The animal was pushed to the end of the loading channel with its dorsal side facing the objective. GCaMP6m signal was recorded using an inverted Nikon Ti-E

spinning disk confocal microscope and a 60X water immersion objective (NA 1.2). A CCD microscope camera (Andor iXon EMCCD) captured frames at 30 Hz. Recordings from at least 5–7 larvae were collected for each condition. For each larva the average response over 5s around the peak value during stimulus presentation was compared to chance level analyzed via normal t-test. Responses during stimulation were normalized based on the baseline response 10s before the stimulation. P-values for each experiment are given in the respective figure panel. Each graph shows the mean calcium signal plotted as the relative response strength $\Delta F/F$ and the related standard error of the mean on the y axis. The time in seconds is given below each graph on the x axis. The grey box indicates the duration of the stimulus application. The sample size of each group (N=5-7) is given above each row. n.s. $p > 0.05$; * $p < 0.05$.

Behavioral Experiments

Associative olfactory learning

Standard experiments were done as described before (Apostolopoulou et al 2013, Gerber et al 2013, Hendel et al 2005, Michels et al 2017, Widmann et al 2018). Learning experiments were conducted on assay plates (85 mm diameter, Sarstedt, cat. no. 82.1472) filled with a thin layer of either 2.5% (w/v) pure agarose solution (Sigma Aldrich, cat. no. A9539) or 2.5% (w/v) agarose plus either 1.5 M sodium chloride solution (VWR Chemicals, cat. no. 27810.364), 2 M D-Fructose solution (Sigma Aldrich cat. no. 47740) or 10 mM quinine solution (quinine hemisulfate; Sigma Aldrich cat. no. Q1250). Before closing and labeling the lids, solutions were let to cool down at room temperature to avoid condensation. Plates were stored at 18°C and used within five days. As olfactory stimuli, we used two different odor combinations: either amyl acetate (AM, Sigma Aldrich, cat. no. 46022) diluted 1:250 in paraffin oil (Sigma Aldrich, cat. no. 76235) and undiluted benzaldehyde (BA, Sigma Aldrich, cat. no. 12010) or benzaldehyde and hexyl acetate (HA, Sigma Aldrich, cat. no. 108154) both diluted 1:100 in

paraffin oil. For both odor combinations, 10 µL odor were loaded into custom-made Teflon containers (4.5 mm diameter) with perforated lids (Scherer et al 2003).

A minimum of 30 early third instar larvae were collected and exposed to a first odor (amyl acetate or hexyl acetate) while crawling on pure agarose for five minutes, followed by five minutes exposition to a second odor (benzaldehyde) on agarose medium with either 1.5 M sodium chloride, 10 mM quinine as negative reinforcer or 2 M D-Fructose as positive reinforcer (Odor1/Odor2+). For three cycle training, two more repetitions of training trials were performed. A second group of larvae received reciprocal training (Odor1+/Odor2). After one or three training cycles, larvae were transferred onto test plates containing either pure agarose (reward learning) or agarose plus salt or quinine (punishment learning) on which odor 1 and odor 2 were represented on opposite sides. After five minutes, larvae were counted on each side of the test plate (#Odor1, #Odor2) or in a 10 mm neutral zone in the middle of the plate (#Neutral). A Preference index (PREF) for each group of larvae was calculated as follows:

$$\mathrm{PREF}_{\mathrm{Odor1/Odor2+}} = \frac{\#\mathrm{Odor2} - \#\mathrm{Odor1}}{\#\mathrm{Total}}$$

$$\mathrm{PREF}_{\mathrm{Odor1+/Odor2}} = \frac{\#\mathrm{Odor1} - \#\mathrm{Odor2}}{\#\mathrm{Total}}$$

To measure specifically the effect of associative learning, we then calculated the associative performance index (PI) as the difference in preference between the reciprocally trained larvae:

$$\mathrm{PI} = \frac{\mathrm{PREF}_{\mathrm{Odor1/Odor2+}} + \mathrm{PREF}_{\mathrm{Odor1+/Odor2}}}{2}$$

Negative Performance Indices represent aversive associated learning, whereas positive values represent appetitive learning. Division by 2 ensures scores are bound within (-1; 1).

Odor preference test

Pure agarose (2.5% w/v) plates were cast as previously described (Apostolopoulou et al 2013, Gerber et al 2013, Michels et al 2017, Scherer et al 2003, Widmann et al 2018). Furthermore, the odors were prepared according to the dilutions used in the learning experiments. An odor container (either AM 1:250, BA undiluted, HA 1:100, or BA 1:100) was placed on one side of the agarose plate. An empty container was placed on the opposite side to exclude visual or other side effects. Approximately 30 third instar feeding stage larvae were collected and placed on the plate for 5 min. After this time, larvae were counted, subdivided into larvae on the odor side (#Odor), larvae on the empty container side (#Empty) and larvae in a 10 mm neutral zone in the middle of the plate, as well as larvae that were on the lid of the Petri dish (#Neutral). Preferences were calculated as follows:

$$\mathrm{PREF}_{\mathrm{Odor/Empty}} = \frac{\#\mathrm{Odor} - \#\mathrm{Empty}}{\#\mathrm{Total}}$$

Positive values indicate a preference for the respective odor, while negative values indicate odor avoidance. The preference tests were performed in different orientations (odor container on plate up/down/left/right) to exclude directional bias.

Gustatory preference test

High salt-dependent choice behavior experiments were performed using standard methods (Hendel et al 2005, Huser et al 2017, Huser et al 2012, Niewalda et al 2008, Selcho et al 2009, Widmann et al 2016). A 2.5% (w/v) agarose solution was boiled as previously described and a thick layer was poured into Petri dishes. After cooling, half of the agarose in the Petri dish was removed and filled by 2.5% (w/v) agarose solution with 1.5 M sodium chloride. For the choice experiment, about 30 third instar feeding stage larvae were put in the middle of the Petri dish and let them crawl for five minutes. Larvae were then counted as being located on the sodium chloride side (#NaCl), pure agarose side (#Agarose), or a neutral area of about 10 mm width in the middle of the plate (#Neutral), as well as larvae that were on the lid of the

Petri dish (#Neutral). The gustatory preference indices for sodium chloride were calculated as follows:

$$\mathrm{PREF}_{\mathrm{NaCl}} = \frac{\#\mathrm{NaCl} - \#\mathrm{Agarose}}{\#\mathrm{Total}}$$

Negatives values for preference indices indicate an aversion to sodium chloride.

Optogenetic substitution experiment

To substitute an actual salt punishment by remotely activating DANs, we used UAS-ChR2^{XXL}. Effector lines were crossed to *w*^{1118} to obtain appropriate genetic controls. Larvae were maintained in vials with *Drosophila* standard food on 25°C and wrapped in aluminum foil to ensure development in constant darkness. A group of 30 feeding-stage third-instar larvae were placed onto plates containing 2.5% agarose and exposed to either AM or BA. During the presentation of the first odor, the larvae were exposed to blue light (470 nm, 2.5 V, 220 lux) for 5 minutes. The second odor BA (undiluted) was presented in darkness for five minutes on a pure agarose plate. As described for odor-high salt learning, training was performed reciprocally and the sequence of training trials was alternated across repetitions of the experiment. Data were then scored as above. Please note, tests were done in the presence of 1.5 M sodium chloride to test for the specific quality of the memory.

Optogenetic inhibition of neuronal activity

To acutely block synaptic output, we used UAS-GtACR2. Flies were maintained on standard food supplemented with 0.5 mM all-*trans*-retinal (ATR, Sigma Aldrich, cat. no. R2500) at 25°C as described before (Meloni et al 2020). Vials were wrapped in aluminum foil to ensure larval development in constant darkness. Groups of about 30 third instar feeding stage larvae

received a reciprocal two-odor training as described before, exposed to blue light (470 nm, 2.7 V, 1100 lux) during the entire training phase. The test was performed for 5 minutes in darkness on an agarose plate mixed with 1.5 M sodium chloride. Control experiments were performed with the same genotype but with standard food lacking 0.5 mM all-*trans*-retinal. Data were then calculated and score as mentioned above.

Evaluation of DAN input wiring diagrams

Pie charts of sensory profiles were calculated using the percentage of total synaptic input of interneurons as fraction (thereby ignoring other inputs to show distribution of sensory origins). Percentages then give the percentage of total sensory synaptic input to interneurons. The calculation of the hub score was done in the following way: Fraction of total synaptic input from all sensory neurons to defined interneurons (see IDs) was multiplied by the total fraction of input of the DANs from this interneuron. For anatomical reconstructions and visualizations included here, we made use of earlier published data (Eichler et al 2017, Eschbach et al 2020, Miroschnikow et al 2018, Winding et al 2023).

Statistical Analysis

Behavioral results were analyzed in GraphPad Prism 8.4.3. To test for normal distribution, Shapiro-Wilk test was applied. Groups that did not violate the assumption of normal distribution, were analyzed with an unpaired t-test (comparison of two groups) or a one-way ANOVA followed by a Tukey's post hoc test (comparisons between groups larger than two). For nonparametric statistics, Mann-Whitney test (comparison between two groups) or Kruskal-Wallis followed by Dunn's multiple comparisons tests were applied. Furthermore, Wilcoxon signed-rank tests were performed to compare medians against chance level. Results are visualized in box-plots, indicating the median as middle line, 25%/75% quantiles as box

boundaries and minimum/maximum performance indices as whiskers. Each data point is represented as black dot and sample sizes are noted within graphics. Asterisks and ‘‘n.s.’’ indicate $p < 0.05$ and $p > 0.05$, respectively.

705

Supplemental Information

Supplemental Information includes Supplemental Experimental Procedures and additional Figures and can be found with this article online.

Acknowledgments

This work was supported by the Deutsche Forschungsgemeinschaft (Grant No. 441181781, 426722269, 432195391) and by EU funds from the ESF Plus Program (Grant No. 100649752) all to AST. KV was supported by a DFG postdoc grant (Grant No. 345729665). We thank Aravi Samuel for continuous support and discussions. We thank Bert Klagges, Tilman Triphan, Dennis Pauls, Mareike Selcho, and Wolf Huetteroth for discussions and comments. Additionally, we thank Juliane Saumweber for fly care and maintenance.

Author contributions

Conceptualization, D.W., K.V., A.M., M.P. and A.S.T; Methodology, D.W., K.V. and A.S.T; Investigation, D.W., K.V., A.M., M.P. and A.S.T; Writing, D.W., K.V., A.M., M.P. and A.S.T; Supervision, D.W. and A.S.T.

Figures

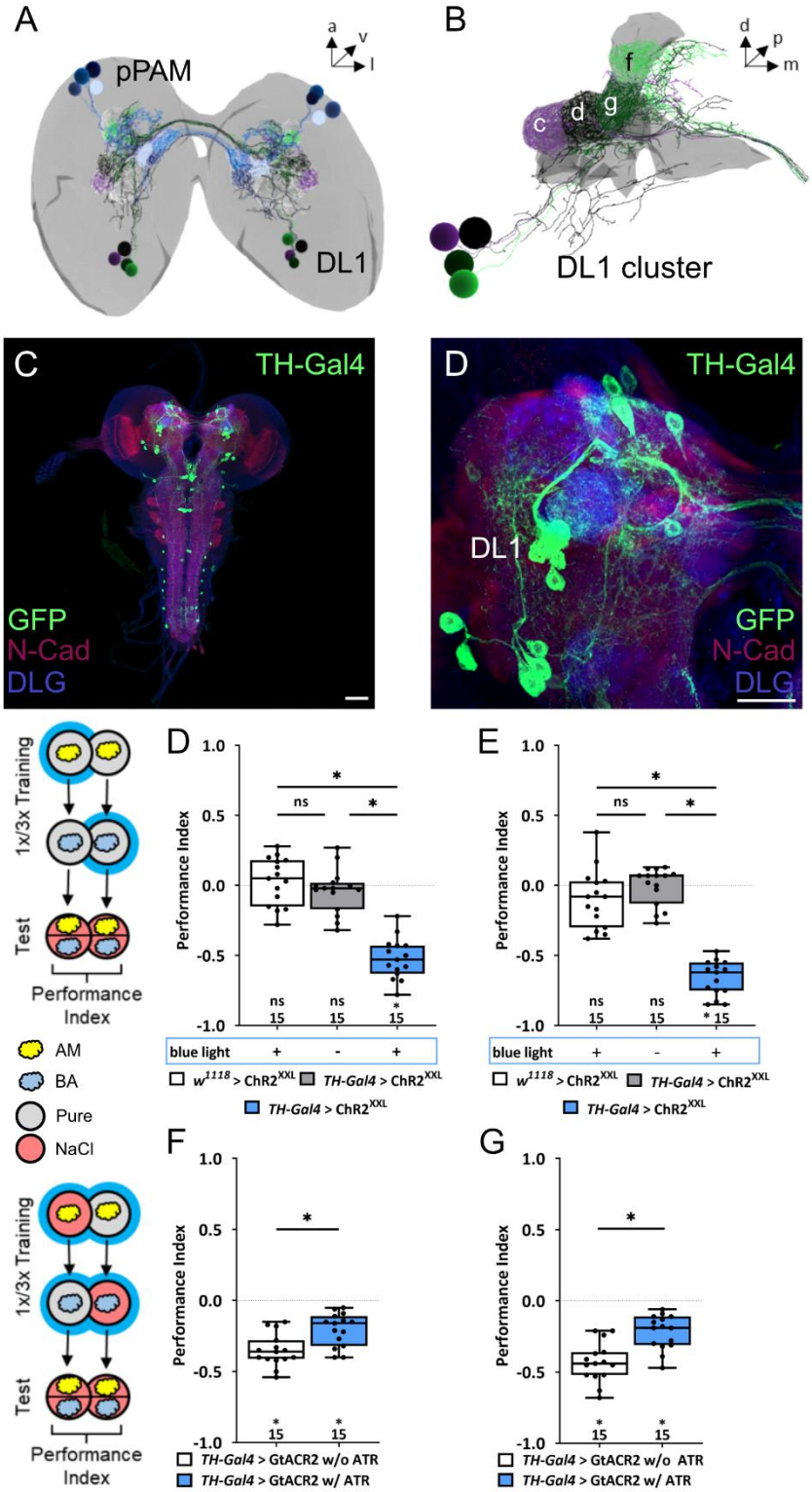

725 **Figure 1: The larval dopaminergic system is subdivided in two functionally distinct clusters. (A)** The larval dopaminergic neurons (DANs) can be anatomically subdivided into the primary protocerebral anterior medial (pPAM) and dorsolateral 1 (DL1) cluster based on

their cell body position. **(B)** The DL1 cluster (cell bodies in green and purple) consists of four DANs providing input to the c, d, g, and f compartment of the vertical lobe, peduncle and lateral appendix of the MB (in grey). **(C, D)** Four DL1 DANs (DAN-c1, DAN-d1, DAN-g1, and DAN-f1) are included in the expression pattern of the TH-GAL4 driver line. However, expression of a UAS-mCD8::GFP reporter via TH-GAL4 labels many more neurons (in green, anti-GFP) throughout the entire CNS (in red and blue, anti-N-cadherin and anti-discs large), in total about 100 neurons. **(E)** To test whether optogenetic activation of the DL1 DANs is sufficient to substitute for a punishment, we used the TH-GAL4 driver in combination with UAS-ChR^{XXL}. Experimental and control larvae were trained by simultaneously presenting and odor and blue light and thus artificial activation of DL1 DANs, whereas a second odor was presented in darkness. Only larvae of the experimental genotype ($p > 0.05$), but not of the two genetic controls (both $p < 0.05$), retrieve an aversive associative olfactory memory. The same result was seen after one or three training trials (**E** and **F**, respectively). **(G, H)** To test for the acute function of the DL1 DANs in aversive associative olfactory memory, we expressed GtACR2 via the TH-GAL4 driver. Acute optogenetic inhibition of synaptic output from DL1 and other DANs reduced odor high salt memory. Experimental larvae raised on supplemented food (0.5 mM all-*trans*-retinal, ATR) and trained in blue light performed on a lower level than control animals kept on standard food ($p < 0.05$). A memory impairment was seen after one and three training trials (**G** and **H**, respectively). All behavioral data is shown as box-plots. Differences between groups are highlighted by horizontal lines between them. Performance indices different from random distribution are indicated below each box-plot. The sample size of each group (N=15) is given below each box-plot. n.s. $p > 0.05$; * $p < 0.05$. Scale bars: in **C** 50 µm and in **D** 25 µm.

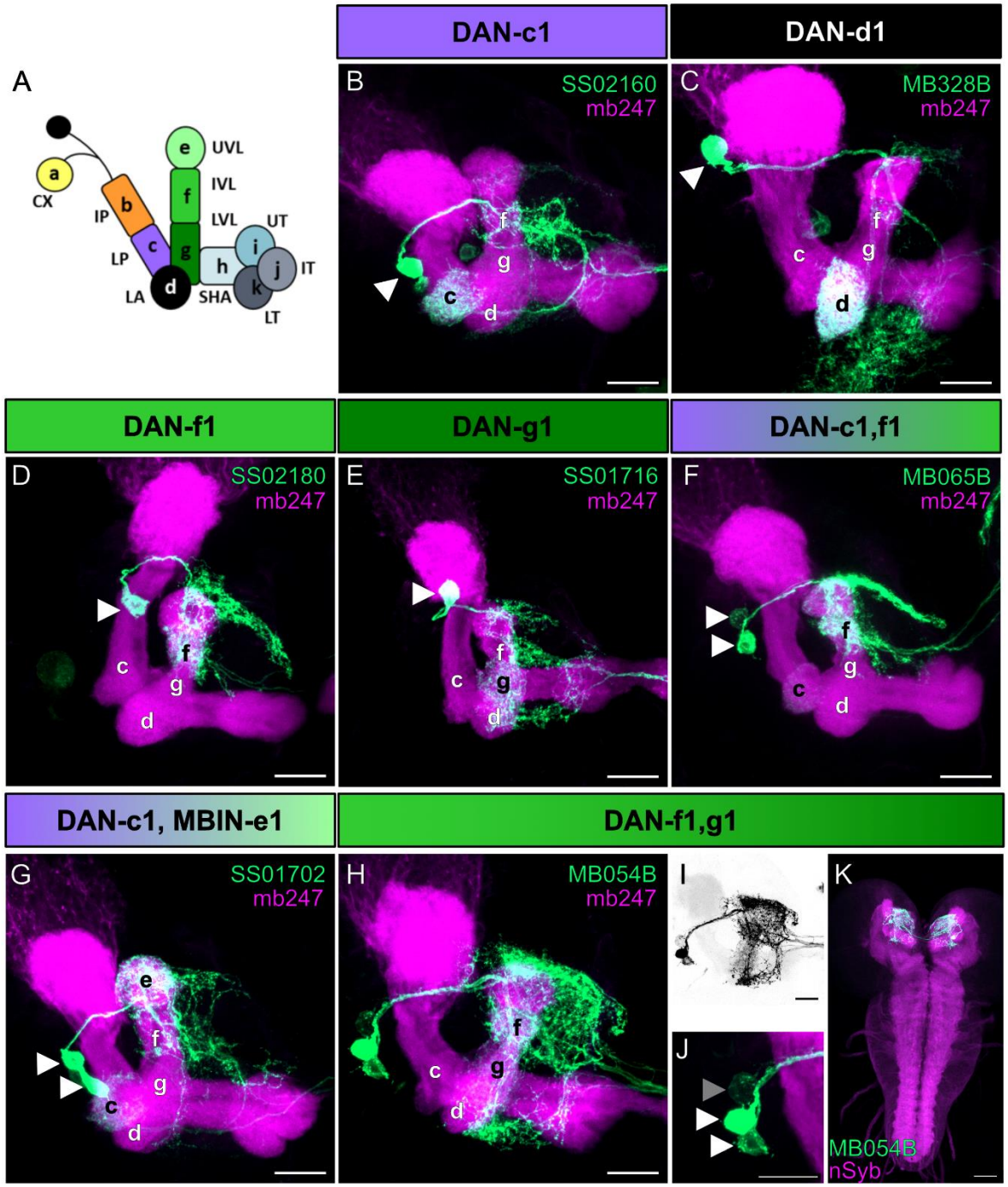

Figure 2: Anatomical single cell analysis of DL1 DAN specific split-GAL4 driver lines. (A) The larval MB is organized into 11 compartments: CX calyx; IP and LP intermediate and lower peduncle; LA lateral appendix; UVL, IVL, and LVL upper, intermediate, and lower vertical
755 lobe; SHA, UT, IT, LT shaft as well as upper, intermediate, and lower toe of the medial lobe. Single-letter synonyms of compartment names are given as “a–k”. These letters are used to indicate compartment innervation by the MB input and output neurons (Saumweber et al

2018). DL1 cluster DANs are DAN-c1, DAN-d1, DAN-g1, and DAN-f1 that innervate the respective four different compartments of the MB. **(B-J)** Individual split-Gal4 driver lines were crossed with the reporter strain UAS-mCD8::GFP;mb247-lexA,lexAop-mRFP. Third instar larval brains were dissected, fixed and mounted to visualize the endogenous expression of the MB reporter (mb247-lexA,lexAop-mRFP shown in magenta) and the respective DAN pattern (GFP shown in green). (B-E) SS02160 (DAN-c1), MB328B (DAN-d1), SS02180 (DAN-f1), SS01716 (DAN-g1) each specifically label a single DL1 DAN (cell bodies are highlighted by white arrowheads). **(F–K)** Two neurons can be seen in MB065B, SS01702, and MB054B split-Gal4 that express in DAN-c1/DAN-f1, DAN-c1/MBIN-e1, and DAN-f1/DAN-g1. Please note that MB065B shows strong expression DAN-f1 but weaker staining in DAN-c1. **(H–K)** MB054B showed reliable strong expression in DAN-f1 and DAN-g1. In some brains a third weak cell body was visible right next to the other two DANs (**I**; GFP channel inverted and shown in black; **J**; cell body highlighted with gray arrowhead). Due to the low expression level we were not able to identify this cell given that only the g and f compartment of the MB were innervated **(H)**. **(K)** Analysis of the entire brain via native fluorescence expression of GFP (green) and n-Syb (magenta) did not reveal additional cells for MB054B split-Gal4. Scale bars: **(B-J)** 20 µm, **(K)** 50µm.

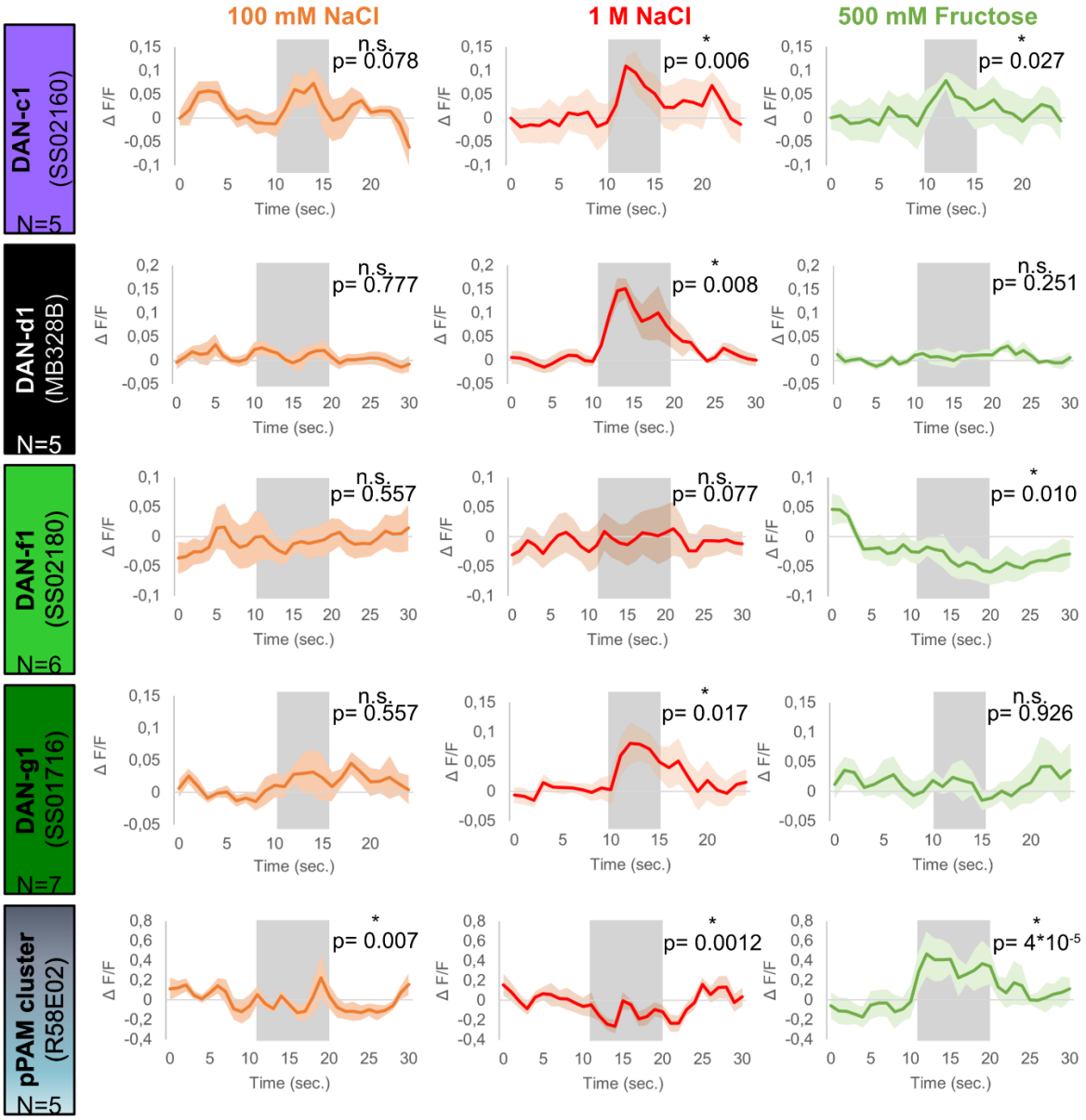

Figure 3: Calcium responses of DANs to gustatory stimulation. Four different split-Gal4 lines and the R58E02 driver line were crossed with UAS-GCaMP6m to express a calcium reporter in DANs. The responses of each DAN towards 100 mM NaCl, 1 M NaCl, and 500 mM fructose was tested in intact larvae using a microfluidic chip-based setup. **(A)** 1 M NaCl (red) and 500 mM fructose (green, $p < 0.05$ for both), but not 100 mM NaCl (orange, $p > 0.05$), induced a calcium response in DAN-c1. **(B)** DAN-d1 calcium responses were only seen after 1 M NaCl stimulation (red, $p < 0.05$), but not after 100 mM NaCl (orange, $p > 0.05$) and 500 mM fructose stimulation (green, $p > 0.05$). **(C)** Stimulation with 100 mM (orange, $p > 0.05$) and 1 M NaCl (red, $p > 0.05$) did not induce calcium responses in DAN-f1. However, stimulation

with 500 mM fructose reduced the obtained calcium signal (green, $p < 0.05$). **(D)** 1 M NaCl (red, $p < 0.05$), but not 100 mM NaCl (orange, $p > 0.05$) and 500 mM fructose (green, $p > 0.05$), induced a calcium response in DAN-g1. **(E)** pPAM DANs calcium responses were only seen after 500 mM fructose stimulation (green, $p < 0.05$). Stimulation with low (orange) and high salt concentrations (red) did not increase calcium signals, however both reduced pPAM activity ($p < 0.05$). Each graph shows the mean calcium signal plotted as the relative response strength $\Delta F/F$ and the related standard error of the mean on the y axis. The time in seconds is given below each graph on the x axis. The grey box indicates the duration of the stimulus application. The sample size of each group (N=5-7) is given above each row. n.s. $p > 0.05$; * $p < 0.05$.

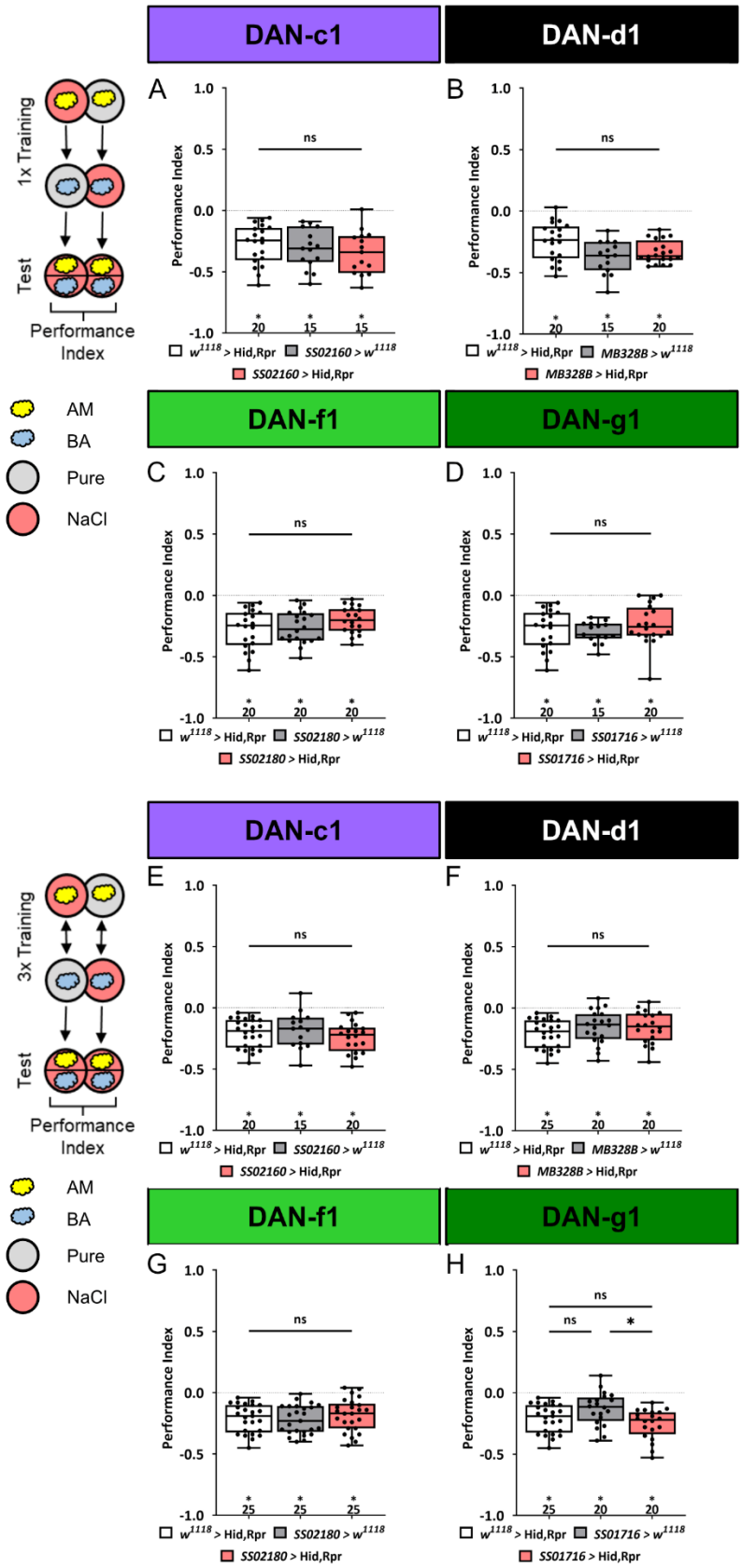

Figure 4: Ablation of individual DANs does not impair aversive olfactory memory. In all panels aversive associative performance indices are shown for tests immediately after odor-

high salt classical conditioning. In the upper panels **(A-D)** larvae are trained once, whereas in the lower panels **(E-H)** three training cycles were applied. Schematic overviews for both conditioning protocols are shown on the left. The four different DL1 DAN specific split-Gal4 driver strains SS02160, MB328B, SS02180, and SS01716 were crossed to the effector UAS-hid,rpr to induce apoptosis **(A-H)**. Cell-specific ablation of distinct DL1 DANs did not impair odor-high salt memories after either one or three cycle training. In no case were associative performance indices upon DL1 DAN ablation lower than in both genetic controls (**A-H**, in all experiments at least one or even both control groups are compared to the experimental group $p > 0.05$). All behavioral data is shown as box-plots. Differences between groups are highlighted by horizontal lines between them. Performance indices different from random distribution are indicated below each box-plot. The sample size of each group (N=15, 20, or 25) is given below each box-plot. n.s. $p > 0.05$; * $p < 0.05$.

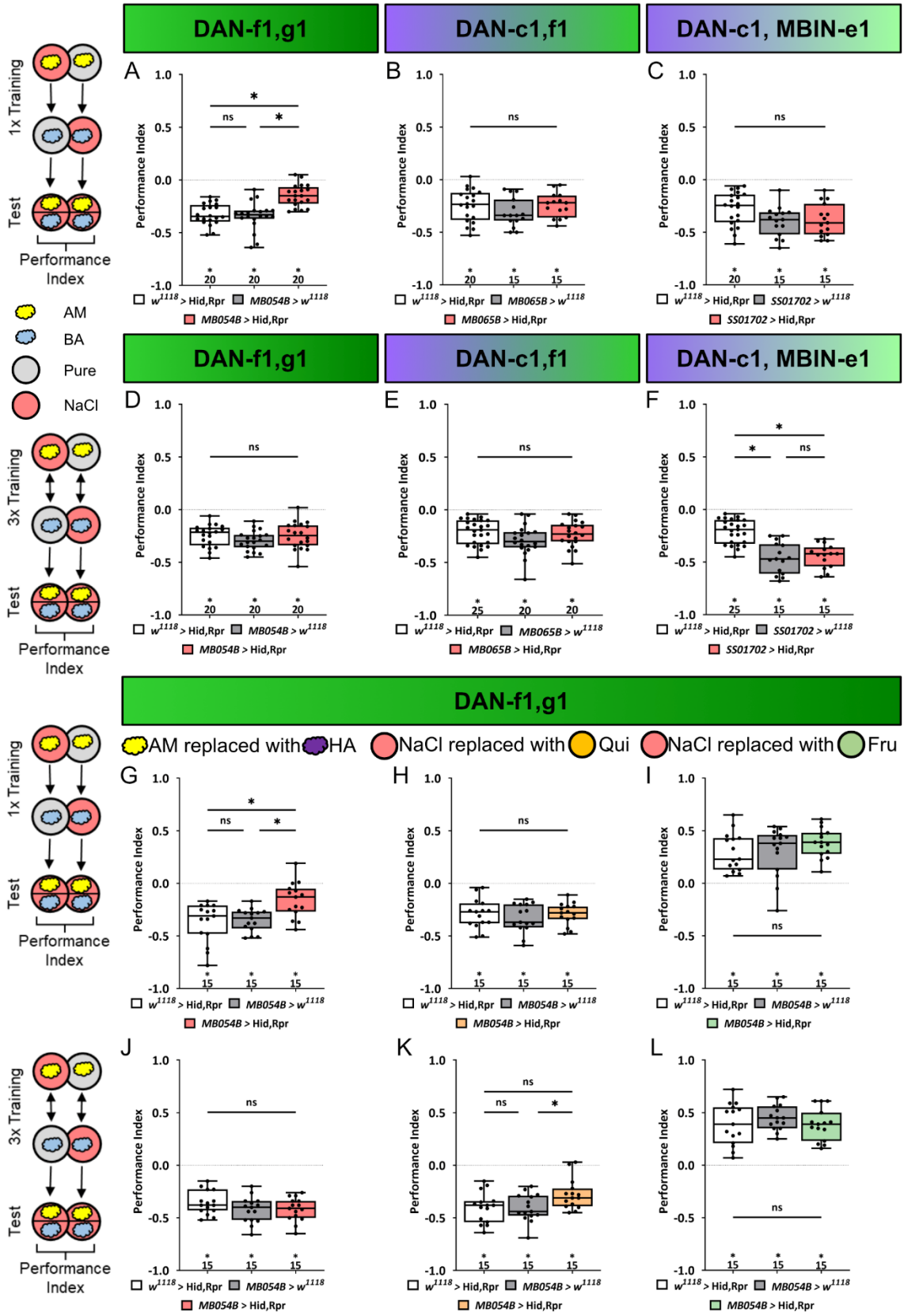

Figure 5: Ablation of DAN-f1 and DAN-g1 together impairs aversive olfactory memory.

In all panels associative performance indices are shown for tests immediately after classical

conditioning. In the upper panels **(A-C)** larvae are trained once by pairing an olfactory stimulus with high salt punishment, whereas in the lower panels **(D-F)** three training cycles were applied. Schematic overviews for both conditioning protocols are shown on the left. The three different DL1 DAN specific split-Gal4 driver MB054B, MB065B, and SS01702 that each label two neurons were crossed to the effector UAS-hid,rpr to induce apoptosis **(A-F)**. (A) With MB054B used as driver strain to ablate the DL1 DAN combination DAN-f1/DAN-g1, the aversive associative performance index of the experimental group was decreased compared to both controls ($p < 0.05$). **(B-F)** In all other experiments ablation of different DL1 DAN combinations did not reveal a phenotype. (in all experiments at least one or even both control groups are compared to the experimental group $p > 0.05$). Please note, that this also includes MB054B crossed with UAS-hid,rpr tested after three training trials **(D)**. **(G)** To verify the memory phenotype of MB054B crossed with UAS-hid,rpr tested after one trail conditioning, we repeated the experiment using the odor pair hexyl acetate (HA) and benzaldehyde (BA). Again, experimental larvae tested after one trial learning showed a robust decrease in odor-high salt memory when compared to both genetic control groups ($p < 0.05$). The memory phenotype was not seen after three training trials (J, $p > 0.05$). **(H, K)** With MB054B used as driver strain to ablate the DL1 DAN combination DAN-f1/DAN-g1, aversive odor-quinine memory was not impaired after one or three cycle conditioning ($p > 0.05$ when comparing experimental and control groups). Similarly, appetitive odor-fructose learning after one and three cycle conditioning was not impaired when ablating DAN-f1/DAN-g1 ($p > 0.05$ when comparing experimental and control groups). All behavioral data is shown as box-plots. Differences between groups are highlighted by horizontal lines between them. Performance indices different from random distribution are indicated below each box-plot. The sample size of each group (N=15, 20, or 25) is given below each box-plot. n.s. $p > 0.05$; * $p < 0.05$.

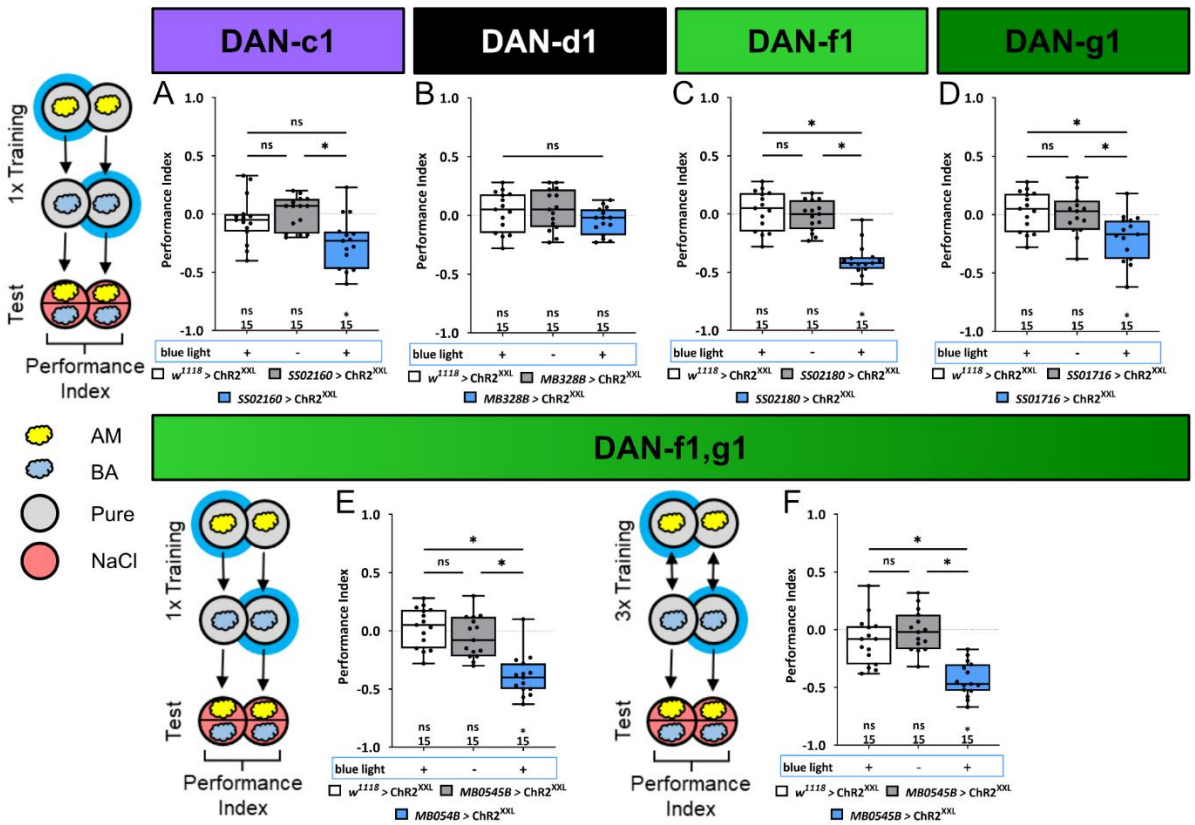

Figure 6: Optogenetic DL1 DAN activity can substitute for salt punishment. In all panels associative performance indices are shown for tests immediately after classical conditioning. In panels **(A-E)** larvae are trained once by pairing an olfactory stimulus with artificial blue light activation, whereas in panel **(F)** three training cycles were applied. Schematic overviews for both conditioning protocols are shown to the left of **(A)** and **(F)**. **(A-D)** To test whether optogenetic activation of the individual DL DANs DAN-c1, DAN-d1, DAN-f1, and DAN-g1 is sufficient to substitute for a punishment, we used the split-Gal4 lines SS02160, MB328B, SS02180, and SS01716 in combination with UAS-ChR2^{XXL}. **(E, F)** For simultaneous optogenetic activation of DAN-f1/DAN-g1 we used MB054B. Larvae of the experimental genotypes for DAN-c1, DAN-f1, DAN-g1 and the DAN-f1/DAN-g1 combination (for all $p < 0.05$), but not for DAN-d1 and all genetic controls (for all $p > 0.05$), showed an aversive associative memory. The results imply that in the tested conditions, the punishment signal can be mediated by the artificial activation of all individual DL1 DANs, with the exception of DAN-d1. All behavioral data is shown as box-plots. Differences between groups are highlighted by horizontal lines between them. Performance indices different from random distribution are

indicated below each box-plot. The sample size of each group (N=15) is given below each box-plot. n.s. $p > 0.05$; * $p < 0.05$.

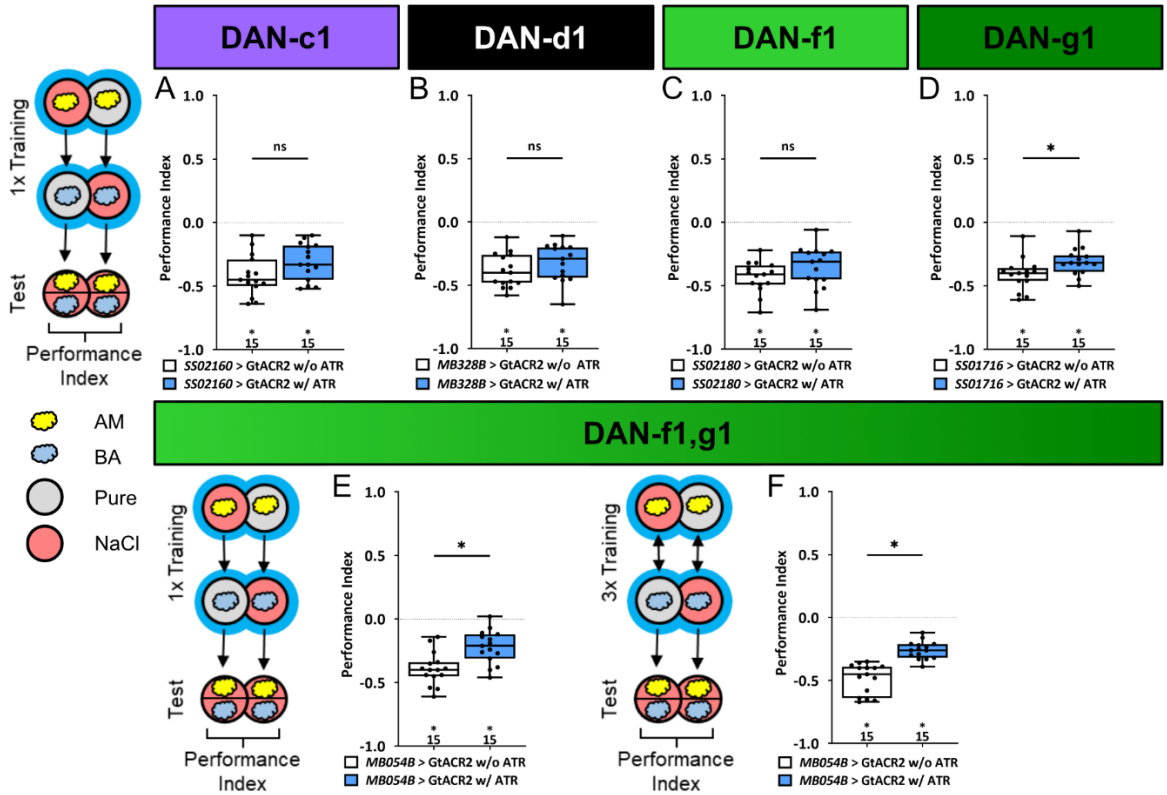

Figure 7: Optogenetic inhibition of DL1 DAN activity impairs aversive olfactory memory. In all panels associative performance indices are shown for tests immediately after classical odor high salt conditioning. In panels **(A-E)** larvae are trained once by pairing an olfactory stimulus with an aversive high salt stimulation, whereas in panel **(F)** three training cycles were applied. Schematic overviews for both conditioning protocols are shown to the left of **(A)** and **(F)**. **(A-D)** To test whether optogenetic inhibition of the individual DL DANs DAN-c1, DAN-d1, DAN-f1, and DAN-g1 during training impairs punishment signaling, we used the split-Gal4 lines SS02160, MB328B, SS02180, and SS01716 in combination with UAS-GtACR2 and blue light stimulation during the entire training phase. **(E, F)** For simultaneous optogenetic inhibition of DAN-f1/DAN-g1 we used MB054B. **(A-C)** Larvae with inhibited DAN-c1, DAN-d1, or DAN-f1 function during training showed no impairment of odor-high salt memory comparable to controls that were kept on standard food without supplemented all-*trans*-retinal (ATR, 0.5 mM) and received the same protocol ($p < 0.05$) (for all $p > 0.05$). **(D-F)** In contrast inhibition of DAN-g1 alone, or the combination of DAN-f1/DAN-g1 after single trial and three trial conditioning impaired odor-high salt memory compared to controls (for all $p < 0.05$). This shows that DAN-

g1 function is of central importance for signaling a salt punishment teaching signal. All behavioral data is shown as box-plots. Differences between groups are highlighted by horizontal lines between them. Performance indices different from random distribution are indicated below each box-plot. The sample size of each group (N=15) is given below each box-plot. n.s. $p > 0.05$; * $p < 0.05$.

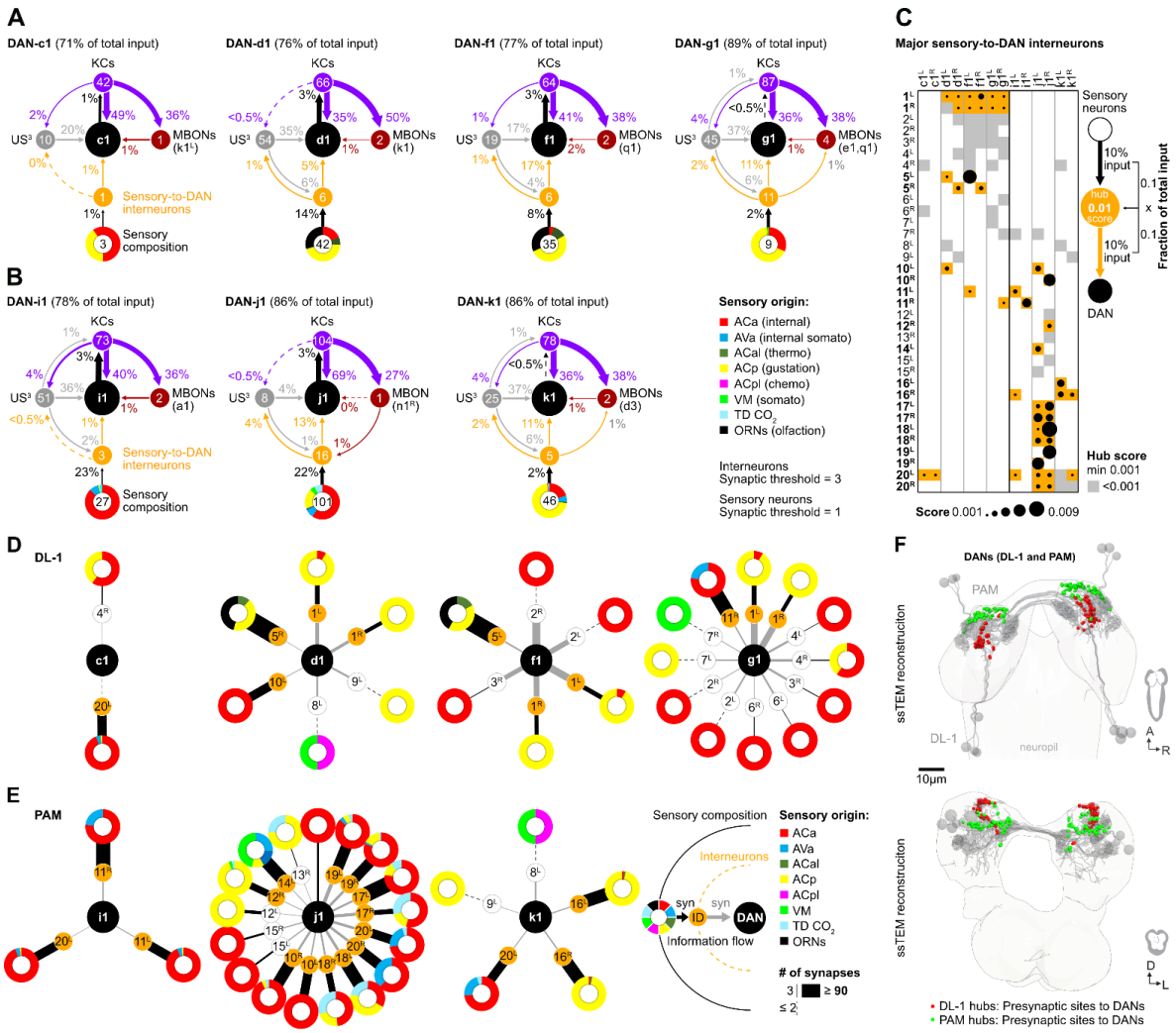

Figure 8: Interneurons and hub analysis of sensory to DAN pathways. (A, B) Schematic graph representation of individual DL1 **(A)** and pPAM **(B)** DANs. The outer ring at the bottom of each scheme represents the sensory composition of neurons targeting sensory-to-DANs interneurons (orange circle). The type of sensory information is encoded by the respective color (ACa: anterior central sensory compartment, AVa: ventral anterior sensory compartment, ACal: lateral anterior central sensory compartment, ACp: posterior anterior central sensory compartment, ACpl: posterior-lateral anterior central sensory compartment, VM: ventromedical sensory compartment, TD CO_2: tracheal dendritic neurons responding to CO_2, ORNs: olfactory receptor neurons). DAN input neurons are shown that get no direct sensory input (grey circles). Individual DANs are shown in the middle of the scheme as black circles. They are connected to MB KC (purple circles), which in turn connect to mushroom body output

neuron (MBONs; dark red circles). Arrows indicate the direction of the synaptic connection and its strength (coded by arrow thickness). Numbers in circles indicate number of neurons. The percentages indicate the proportion relative to the total input that the cell receives from the specific neuronal partners. For example, DAN-f1 receives 17% of its input from six different sensory-to-DAN interneurons (yellow circle), 17% from 19 other, non-sensory interneurons, 41% from 64 MB KCs, and 2% from two MBONs. **(C)** Dot plot showing the importance of interneurons acting as sensory to DAN hub. Dot size was calculated using the fraction of total input an interneuron receives from sensory neurons multiplied by the fraction of total input this interneuron gives to an DAN. Colored backgrounds of dots are highlighted in orange for the connections with a hub size of 0.001 or above. **(D, E)** Schematic of graph representation. The outer ring represents the sensory composition of neurons targeting upstream neurons of DANs. The type of sensory information is encoded by the respective color. Synaptic threshold for upstream interneurons of DANs = 3 and of upstream sensory neurons = 1. Line thickness to interneurons and targets represents the percentage of synaptic input. White or orange circles connected to the outer ring represent the interneuron layer. The inner ring represents individual target neurons, DL1 and pPAM DANs. The identity of each DAN and interneuron is given by the label in its related circle. **(F)** EM reconstruction of DL1 and pPAM DANs (grey) highlighting their presynaptic sites in red (for DL1 DANs) and green (for pPAM DANs). At the top a horizontal view of the brain is shown. At the bottom a frontal view of the brain is shown.

Table 1: A summary of the characteristics of the individual DL1 DANs.

		DAN-c1	DAN-d1	DAN-f1	DAN-g1
Behavior	DAN ablation	No	No	No	No
	DAN substitution	No	No	Yes	Yes
	DAN inhibition	No	No	No	Yes
Physiology		NaCl↑ Fructose↑	NaCl↑	Fructose↓	NaCl↑
Connectomics		# of sensory-to-DAN interneurons			

References

Abbott MK, Lengyel JA. 1991. Embryonic head involution and rotation of male terminalia require the Drosophila locus head involution defective. *Genetics* 129: 783-9

Aceves-Pina EO, Quinn WG. 1979. Learning in normal and mutant Drosophila larvae. *Science* 206: 93-6

Almeida-Carvalho MJ, Berh D, Braun A, Chen YC, Eichler K, et al. 2017. The Ol1mpiad: concordance of behavioural faculties of stage 1 and stage 3 Drosophila larvae. *J Exp Biol* 220: 2452-75

Apostolopoulou AA, Kohn S, Stehle B, Lutz M, Wust A, et al. 2016. Caffeine Taste Signaling in Drosophila Larvae. *Front Cell Neurosci* 10: 193

Apostolopoulou AA, Mazija L, Wust A, Thum AS. 2014. The neuronal and molecular basis of quinine-dependent bitter taste signaling in Drosophila larvae. *Front Behav Neurosci* 8: 6

Apostolopoulou AA, Widmann A, Rohwedder A, Pfitzenmaier JE, Thum AS. 2013. Appetitive associative olfactory learning in Drosophila larvae. *J Vis Exp*

Aso Y, Hattori D, Yu Y, Johnston RM, Iyer NA, et al. 2014. The neuronal architecture of the mushroom body provides a logic for associative learning. *Elife* 3: e04577

Aso Y, Herb A, Ogueta M, Siwanowicz I, Templier T, et al. 2012. Three dopamine pathways induce aversive odor memories with different stability. *PLoS Genet* 8: e1002768

Aso Y, Rubin GM. 2016. Dopaminergic neurons write and update memories with cell-type-specific rules. *Elife* 5

Aso Y, Siwanowicz I, Bracker L, Ito K, Kitamoto T, Tanimoto H. 2010. Specific dopaminergic neurons for the formation of labile aversive memory. *Curr Biol* 20: 1445-51

Berck ME, Khandelwal A, Claus L, Hernandez-Nunez L, Si G, et al. 2016. The wiring diagram of a glomerular olfactory system. *Elife* 5

Berry JA, Cervantes-Sandoval I, Chakraborty M, Davis RL. 2015. Sleep Facilitates Memory by Blocking Dopamine Neuron-Mediated Forgetting. *Cell* 161: 1656-67

Berry JA, Phan A, Davis RL. 2018. Dopamine Neurons Mediate Learning and Forgetting through Bidirectional Modulation of a Memory Trace. *Cell Rep* 25: 651-62 e5

Burke CJ, Huetteroth W, Owald D, Perisse E, Krashes MJ, et al. 2012. Layered reward signalling through octopamine and dopamine in Drosophila. *Nature* 492: 433-7

Chen TW, Wardill TJ, Sun Y, Pulver SR, Renninger SL, et al. 2013. Ultrasensitive fluorescent proteins for imaging neuronal activity. *Nature* 499: 295-300

Claridge-Chang A, Roorda RD, Vrontou E, Sjulson L, Li H, et al. 2009. Writing memories with light-addressable reinforcement circuitry. *Cell* 139: 405-15

Cognigni P, Felsenberg J, Waddell S. 2018. Do the right thing: neural network mechanisms of memory formation, expression and update in Drosophila. *Curr Opin Neurobiol* 49: 51-58

Das G, Klappenbach M, Vrontou E, Perisse E, Clark CM, et al. 2014. Drosophila learn opposing components of a compound food stimulus. *Curr Biol* 24: 1723-30

Dawydow A, Gueta R, Ljaschenko D, Ullrich S, Hermann M, et al. 2014. Channelrhodopsin-2-XXL, a powerful optogenetic tool for low-light applications. *Proc Natl Acad Sci U S A* 111: 13972-7

Dietzl G, Chen D, Schnorrer F, Su KC, Barinova Y, et al. 2007. A genome-wide transgenic RNAi library for conditional gene inactivation in Drosophila. *Nature* 448: 151-6

Dumstrei K, Wang F, Nassif C, Hartenstein V. 2003. Early development of the Drosophila brain: V. Pattern of postembryonic neuronal lineages expressing DE-cadherin. *J Comp Neurol* 455: 451-62

Eichler K, Li F, Litwin-Kumar A, Park Y, Andrade I, et al. 2017. The complete connectome of a learning and memory centre in an insect brain. *Nature* 548: 175-82

El-Keredy A, Schleyer M, Konig C, Ekim A, Gerber B. 2012. Behavioural analyses of quinine processing in choice, feeding and learning of larval Drosophila. *PLoS One* 7: e40525

Eschbach C, Cano C, Haberkern H, Schraut K, Guan C, et al. 2011. Associative learning between odorants and mechanosensory punishment in larval Drosophila. *J Exp Biol* 214: 3897-905

Eschbach C, Fushiki A, Winding M, Schneider-Mizell CM, Shao M, et al. 2020. Recurrent architecture for adaptive regulation of learning in the insect brain. *Nat Neurosci* 23: 544-55

Felsenberg J, Barnstedt O, Cognigni P, Lin S, Waddell S. 2017. Re-evaluation of learned information in Drosophila. *Nature* 544: 240-44

Fishilevich E, Domingos AI, Asahina K, Naef F, Vosshall LB, Louis M. 2005. Chemotaxis behavior mediated by single larval olfactory neurons in Drosophila. *Curr Biol* 15: 2086-96

Frick A, Bjorkstrand J, Lubberink M, Eriksson A, Fredrikson M, Ahs F. 2022. Dopamine and fear memory formation in the human amygdala. *Mol Psychiatry* 27: 1704-11

Friggi-Grelin F, Coulom H, Meller M, Gomez D, Hirsh J, Birman S. 2003. Targeted gene expression in Drosophila dopaminergic cells using regulatory sequences from tyrosine hydroxylase. *J Neurobiol* 54: 618-27

Galili DS, Dylla KV, Ludke A, Friedrich AB, Yamagata N, et al. 2014. Converging circuits mediate temperature and shock aversive olfactory conditioning in Drosophila. *Curr Biol* 24: 1712-22

Gerber B, Biernacki R, Thum J. 2013. Odor-taste learning assays in Drosophila larvae. *Cold Spring Harb Protoc* 2013

Gerber B, Hendel T. 2006. Outcome expectations drive learned behaviour in larval Drosophila. *Proc Biol Sci* 273: 2965-8

Gerber B, Stocker RF, Tanimura T, Thum AS. 2009. Smelling, tasting, learning: Drosophila as a study case. *Results Probl Cell Differ* 47: 139-85

Glanzman DL. 1995. The cellular basis of classical conditioning in Aplysia californica--it's less simple than you think. *Trends Neurosci* 18: 30-6

Groessl F, Munsch T, Meis S, Griessner J, Kaczanowska J, et al. 2018. Dorsal tegmental dopamine neurons gate associative learning of fear. *Nat Neurosci* 21: 952-62

Heisenberg M. 2003. Mushroom body memoir: from maps to models. *Nat Rev Neurosci* 4: 266-75

Hendel T, Michels B, Neuser K, Schipanski A, Kaun K, et al. 2005. The carrot, not the stick: appetitive rather than aversive gustatory stimuli support associative olfactory learning in individually assayed Drosophila larvae. *J Comp Physiol A Neuroethol Sens Neural Behav Physiol* 191: 265-79

Huetteroth W, Perisse E, Lin S, Klappenbach M, Burke C, Waddell S. 2015. Sweet taste and nutrient value subdivide rewarding dopaminergic neurons in Drosophila. *Curr Biol* 25: 751-58

Huser A, Eschment M, Gullu N, Collins KAN, Bopple K, et al. 2017. Anatomy and behavioral function of serotonin receptors in Drosophila melanogaster larvae. *PLoS One* 12: e0181865

Huser A, Rohwedder A, Apostolopoulou AA, Widmann A, Pfitzenmaier JE, et al. 2012. The serotonergic central nervous system of the Drosophila larva: anatomy and behavioral function. *PLoS One* 7: e47518

Hwang RY, Zhong L, Xu Y, Johnson T, Zhang F, et al. 2007. Nociceptive neurons protect Drosophila larvae from parasitoid wasps. *Curr Biol* 17: 2105-16

Jacob PF, Vargas-Gutierrez P, Okray Z, Vietti-Michelina S, Felsenberg J, Waddell S. 2021. Prior experience conditionally inhibits the expression of new learning in Drosophila. *Curr Biol*

Jovanic T, Schneider-Mizell CM, Shao M, Masson JB, Denisov G, et al. 2016. Competitive Disinhibition Mediates Behavioral Choice and Sequences in Drosophila. *Cell* 167: 858-70 e19

Kacsoh BZ, Bozler J, Hodge S, Ramaswami M, Bosco G. 2015. A novel paradigm for nonassociative long-term memory in Drosophila: predator-induced changes in oviposition behavior. *Genetics* 199: 1143-57

Khurana S, Abu Baker MB, Siddiqi O. 2009. Odour avoidance learning in the larva of Drosophila melanogaster. *J Biosci* 34: 621-31
Khurana S, Robinson BG, Wang Z, Shropshire WC, Zhong AC, et al. 2012. Olfactory conditioning in the third instar larvae of Drosophila melanogaster using heat shock reinforcement. *Behav Genet* 42: 151-61
Kirkhart C, Scott K. 2015. Gustatory learning and processing in the Drosophila mushroom bodies. *J Neurosci* 35: 5950-8
Konig C, Khalili A, Niewalda T, Gao S, Gerber B. 2019. An optogenetic analogue of second-order reinforcement in Drosophila. *Biol Lett* 15: 20190084
Krashes MJ, DasGupta S, Vreede A, White B, Armstrong JD, Waddell S. 2009. A neural circuit mechanism integrating motivational state with memory expression in Drosophila. *Cell* 139: 416-27
Kreher SA, Kwon JY, Carlson JR. 2005. The molecular basis of odor coding in the Drosophila larva. *Neuron* 46: 445-56
Lammel S, Lim BK, Ran C, Huang KW, Betley MJ, et al. 2012. Input-specific control of reward and aversion in the ventral tegmental area. *Nature* 491: 212-7
Li HH, Kroll JR, Lennox SM, Ogundeyi O, Jeter J, et al. 2014. A GAL4 driver resource for developmental and behavioral studies on the larval CNS of Drosophila. *Cell Rep* 8: 897-908
Liu C, Placais PY, Yamagata N, Pfeiffer BD, Aso Y, et al. 2012. A subset of dopamine neurons signals reward for odour memory in Drosophila. *Nature* 488: 512-6
Mancini N, Hranova S, Weber J, Weiglein A, Schleyer M, et al. 2019. Reversal learning in Drosophila larvae. *Learn Mem* 26: 424-35
Masuda-Nakagawa LM, Gendre N, O'Kane CJ, Stocker RF. 2009. Localized olfactory representation in mushroom bodies of Drosophila larvae. *Proc Natl Acad Sci U S A* 106: 10314-9
McCurdy LY, Sareen P, Davoudian PA, Nitabach MN. 2021. Dopaminergic mechanism underlying reward-encoding of punishment omission during reversal learning in Drosophila. *Nat Commun* 12: 1115
Meloni I, Sachidanandan D, Thum AS, Kittel RJ, Murawski C. 2020. Controlling the behaviour of Drosophila melanogaster via smartphone optogenetics. *Sci Rep* 10: 17614
Menegas W, Akiti K, Amo R, Uchida N, Watabe-Uchida M. 2018. Dopamine neurons projecting to the posterior striatum reinforce avoidance of threatening stimuli. *Nat Neurosci* 21: 1421-30
Menzel R. 2001. Searching for the memory trace in a mini-brain, the honeybee. *Learn Mem* 8: 53-62
Menzel R. 2022. In Search for the Retrievable Memory Trace in an Insect Brain. *Front Syst Neurosci* 16: 876376
Michels B, Saumweber T, Biernacki R, Thum J, Glasgow RDV, et al. 2017. Pavlovian Conditioning of Larval Drosophila: An Illustrated, Multilingual, Hands-On Manual for Odor-Taste Associative Learning in Maggots. *Front Behav Neurosci* 11: 45
Miroschnikow A, Schlegel P, Schoofs A, Hueckesfeld S, Li F, et al. 2018. Convergence of monosynaptic and polysynaptic sensory paths onto common motor outputs in a Drosophila feeding connectome. *Elife* 7
Mohammad F, Stewart JC, Ott S, Chlebikova K, Chua JY, et al. 2017. Optogenetic inhibition of behavior with anion channelrhodopsins. *Nat Methods* 14: 271-74
Niewalda T, Singhal N, Fiala A, Saumweber T, Wegener S, Gerber B. 2008. Salt processing in larval Drosophila: choice, feeding, and learning shift from appetitive to aversive in a concentration-dependent way. *Chem Senses* 33: 685-92
Ohyama T, Schneider-Mizell CM, Fetter RD, Aleman JV, Franconville R, et al. 2015. A multilevel multimodal circuit enhances action selection in Drosophila. *Nature* 520: 633-9

Paranjpe P, Rodrigues V, VijayRaghavan K, Ramaswami M. 2012. Gustatory habituation in Drosophila relies on rutabaga (adenylate cyclase)-dependent plasticity of GABAergic inhibitory neurons. *Learn Mem* 19: 627-35
Pauls D, Pfitzenmaier JE, Krebs-Wheaton R, Selcho M, Stocker RF, Thum AS. 2010. Electric shock-induced associative olfactory learning in Drosophila larvae. *Chem Senses* 35: 335-46
Pavlov I. 1927. *Conditioned reflexes: An investigation of the physiological activity of the cerebral cortex*. London: Oxford University Press.
Perkins LA, Holderbaum L, Tao R, Hu Y, Sopko R, et al. 2015. The Transgenic RNAi Project at Harvard Medical School: Resources and Validation. *Genetics* 201: 843-52
Pfeiffer BD, Ngo TT, Hibbard KL, Murphy C, Jenett A, et al. 2010. Refinement of tools for targeted gene expression in Drosophila. *Genetics* 186: 735-55
Pitman JL, Huetteroth W, Burke CJ, Krashes MJ, Lai SL, et al. 2011. A pair of inhibitory neurons are required to sustain labile memory in the Drosophila mushroom body. *Curr Biol* 21: 855-61
Placais PY, Trannoy S, Isabel G, Aso Y, Siwanowicz I, et al. 2012. Slow oscillations in two pairs of dopaminergic neurons gate long-term memory formation in Drosophila. *Nat Neurosci* 15: 592-9
Port F, Strein C, Stricker M, Rauscher B, Heigwer F, et al. 2020. A large-scale resource for tissue-specific CRISPR mutagenesis in Drosophila. *Elife* 9
Ramaekers A, Magnenat E, Marin EC, Gendre N, Jefferis GS, et al. 2005. Glomerular maps without cellular redundancy at successive levels of the Drosophila larval olfactory circuit. *Curr Biol* 15: 982-92
Riabinina O, Luginbuhl D, Marr E, Liu S, Wu MN, et al. 2015. Improved and expanded Q-system reagents for genetic manipulations. *Nat Methods* 12: 219-22, 5 p following 22
Rohwedder A, Wenz NL, Stehle B, Huser A, Yamagata N, et al. 2016. Four Individually Identified Paired Dopamine Neurons Signal Reward in Larval Drosophila. *Curr Biol* 26: 661-9
Saumweber T, Rohwedder A, Schleyer M, Eichler K, Chen YC, et al. 2018. Functional architecture of reward learning in mushroom body extrinsic neurons of larval Drosophila. *Nat Commun* 9: 1104
Scherer S, Stocker RF, Gerber B. 2003. Olfactory learning in individually assayed Drosophila larvae. *Learn Mem* 10: 217-25
Schleyer M, Miura D, Tanimura T, Gerber B. 2015. Learning the specific quality of taste reinforcement in larval Drosophila. *Elife* 4
Schleyer M, Weiglein A, Thoener J, Strauch M, Hartenstein V, et al. 2020. Identification of Dopaminergic Neurons That Can Both Establish Associative Memory and Acutely Terminate Its Behavioral Expression. *J Neurosci* 40: 5990-6006
Schnitzer M, Huang C, Luo J, Je Woo S, Roitman L, et al. 2023. Dopamine signals integrate innate and learnt valences to regulate memory dynamics. *Research Square*
Schroll C, Riemensperger T, Bucher D, Ehmer J, Voller T, et al. 2006. Light-induced activation of distinct modulatory neurons triggers appetitive or aversive learning in Drosophila larvae. *Curr Biol* 16: 1741-7
Schultz W. 2015. Neuronal Reward and Decision Signals: From Theories to Data. *Physiological reviews* 95: 853-951
Selcho M, Pauls D, Han KA, Stocker RF, Thum AS. 2009. The role of dopamine in Drosophila larval classical olfactory conditioning. *PLoS One* 4: e5897
Si G, Kanwal JK, Hu Y, Tabone CJ, Baron J, et al. 2019. Structured Odorant Response Patterns across a Complete Olfactory Receptor Neuron Population. *Neuron* 101: 950-62 e7
Siju KP, Stih V, Aimon S, Gjorgjieva J, Portugues R, Grunwald Kadow IC. 2020. Valence and State-Dependent Population Coding in Dopaminergic Neurons in the Fly Mushroom Body. *Curr Biol* 30: 2104-15 e4
Strausfeld NJ, Hansen L, Li Y, Gomez RS, Ito K. 1998. Evolution, discovery, and interpretations of arthropod mushroom bodies. *Learn Mem* 5: 11-37

Strausfeld NJ, Wolff GH, Sayre ME. 2020. Mushroom body evolution demonstrates homology and divergence across Pancrustacea. *Elife* 9
Tabone CJ, de Belle JS. 2011. Second-order conditioning in Drosophila. *Learn Mem* 18: 250-3
Thum AS, Gerber B. 2019. Connectomics and function of a memory network: the mushroom body of larval Drosophila. *Curr Opin Neurobiol* 54: 146-54
Tian J, Huang R, Cohen JY, Osakada F, Kobak D, et al. 2016. Distributed and Mixed Information in Monosynaptic Inputs to Dopamine Neurons. *Neuron* 91: 1374-89
Tomchik SM. 2013. Dopaminergic neurons encode a distributed, asymmetric representation of temperature in Drosophila. *J Neurosci* 33: 2166-76a
Tomer R, Denes AS, Tessmar-Raible K, Arendt D. 2010. Profiling by image registration reveals common origin of annelid mushroom bodies and vertebrate pallium. *Cell* 142: 800-9
Tracey WD, Jr., Wilson RI, Laurent G, Benzer S. 2003. painless, a Drosophila gene essential for nociception. *Cell* 113: 261-73
Truman JW, Price J, Miyares RL, Lee T. 2023. Metamorphosis of memory circuits in Drosophila reveals a strategy for evolving a larval brain. *Elife* 12
Tsai HC, Zhang F, Adamantidis A, Stuber GD, Bonci A, et al. 2009. Phasic firing in dopaminergic neurons is sufficient for behavioral conditioning. *Science* 324: 1080-4
Villar ME, Pavao-Delgado M, Amigo M, Jacob PF, Merabet N, et al. 2022. Differential coding of absolute and relative aversive value in the Drosophila brain. *Curr Biol* 32: 4576-92 e5
von Essen AM, Pauls D, Thum AS, Sprecher SG. 2011. Capacity of visual classical conditioning in Drosophila larvae. *Behav Neurosci* 125: 921-9
Vrontou E, Groschner LN, Szydlowski S, Brain R, Krebbers A, Miesenbock G. 2021. Response competition between neurons and antineurons in the mushroom body. *Curr Biol* 31: 4911-22 e4
Waddell S. 2013. Reinforcement signalling in Drosophila; dopamine does it all after all. *Curr Opin Neurobiol* 23: 324-9
Watabe-Uchida M, Eshel N, Uchida N. 2017. Neural Circuitry of Reward Prediction Error. *Annu Rev Neurosci* 40: 373-94
Weber D, Richter V, Rohwedder A, Grossjohann A, Thum AS. 2023a. The Analysis of Aversive Olfactory-Taste Learning and Memory in Drosophila Larvae. *Cold Spring Harb Protoc* 2023: pdb prot108050
Weber D, Richter V, Rohwedder A, Grossjohann A, Thum AS. 2023b. Learning and Memory in Drosophila Larvae. *Cold Spring Harb Protoc* 2023: pdb top107863
Weiglein A, Thoener J, Feldbruegge I, Warzog L, Mancini N, et al. 2021. Aversive teaching signals from individual dopamine neurons in larval Drosophila show qualitative differences in their temporal "fingerprint". *J Comp Neurol* 529: 1553-70
White K, Tahaoglu E, Steller H. 1996. Cell killing by the Drosophila gene reaper. *Science* 271: 805-7
Widmann A, Artinger M, Biesinger L, Boepple K, Peters C, et al. 2016. Genetic Dissection of Aversive Associative Olfactory Learning and Memory in Drosophila Larvae. *PLoS Genet* 12: e1006378
Widmann A, Eichler K, Selcho M, Thum AS, Pauls D. 2018. Odor-taste learning in Drosophila larvae. *J Insect Physiol* 106: 47-54
Winding M, Pedigo BD, Barnes CL, Patsolic HG, Park Y, et al. 2023. The connectome of an insect brain. *Science* 379: eadd9330
Yamada D, Bushey D, Li F, Hibbard KL, Sammons M, et al. 2023. Hierarchical architecture of dopaminergic circuits enables second-order conditioning in Drosophila. *Elife* 12
Yamagata N, Ichinose T, Aso Y, Placais PY, Friedrich AB, et al. 2015. Distinct dopamine neurons mediate reward signals for short- and long-term memories. *Proc Natl Acad Sci U S A* 112: 578-83